Optimizing the production procedure of ball milled Magnesium-Nickel powders for hydrogen storage applications

A Thesis Submitted to the

College of Graduate and Postdoctoral Studies in Partial Fulfillment of the

Requirements for the Degree of Master of Science

In the Department of Mechanical Engineering

University of Saskatchewan

Saskatoon

By

Bhaskar Paliwal

PERMISSION TO USE

In presenting this thesis in partial fulfillment of the requirements for a Postgraduate degree from the University of Saskatchewan, I agree that the Libraries of this University may make it freely available for inspection. I further agree that permission for copying of this thesis/dissertation in any manner, in whole or in part, for scholarly purposes may be granted by the professor or professors who supervised my thesis/dissertation work or, in their absence, by the Head of the Department or the Dean of the College in which my thesis work was done. It is understood that any copying or publication or use of this thesis/dissertation or parts thereof for financial gain shall not be allowed without my written permission. It is also understood that due recognition shall be given to me and to the University of Saskatchewan in any scholarly use which may be made of any material in my thesis.

Requests for permission to copy or to make other use of material in this thesis in whole or part should be addressed to:

Head of the Department of Mechanical Engineering
57 Campus Drive
University of Saskatchewan
Saskatoon, Saskatchewan S7N 5A9
Canada

OR

Dean
College of Graduate and Postdoctoral Studies
University of Saskatchewan
116 Thorvaldson Building, 110 Science Place
Saskatoon, Saskatchewan S7N 5C9
Canada

ABSTRACT

With the advent of time and growing world population, the demand of energy is rising everyday exponentially. Developing renewable sources is important in fulfilling a part of our present energy demands. However, at present, a very significant part of energy is derived from the fossil fuels. Using fossil fuels as the main source of energy has some serious drawbacks.

Fossil fuels are present in the earth's crust in a limited amount and will be exhausted at some point of time. Also, burning fossil fuels to produce energy is responsible for the rising levels of carbon dioxide in the earth's atmosphere. This has led to environmental issues such as the global warming. Hydrogen is a potential alternative to fossil fuels due to its high calorific value and cleaner combustion. The major issue in using hydrogen as a fuel is its storage. Amongst different materials, magnesium is the most suitable candidate for storing hydrogen due to its high theoretical hydrogen storage estimated value (7.5wt%) and economical cost.

Magnesium however has slow reaction kinetics therefore various methods have been investigated to improve its hydrogen storage capacity and reaction kinetics.

In this thesis the effect of different parameters (ball milling time, nickel percentage, hydrogen charging pressure and hydrogen charging temperature) in the production of Magnesium-Nickel powders for the storage of hydrogen were studied. The phase distribution, particle size and morphology were also determined by using scanning electron microscopy, energy dispersive spectroscopy and X-ray diffraction. It was established that Mg-10%Ni ball milled for 10hours, charged at a hydrogen pressure and temperature of 20 bar and at 300 °C respectively was the best sample in terms of the amount of hydrogen stored (≈ 5.6 weight percent) and the hydrogen discharge rate. Cross-sectional SEM and EDS scans revealed that upon ball milling for 10 hours the internal structure of the particles became layered, hosting numerous potential sites for the hydrogen atom residence. It was also clear that the distribution of nickel over magnesium particles was uniform when ball milled for 10 hours.

ACKNOWLEDGMENT

I would like to thank my supervisor Prof. Jerzy A Szpunar for his leadership and encouragement. This research would not have been successful without his support.

I would also like to acknowledge the support from the Department of Mechanical Engineering faculty and staff, my committee members; Prof. Chris Zhang and Prof. Scott Noble. Lastly, I would like to appreciate the support from my colleagues in Prof. Szpunar's research group especially Dr. Salman Razavi for his immense support and guidance throughout this research.

DEDICATION

I DEDICATE THIS THESIS TO MY BELOVED PARENTS FOR THEIR UNCONDITIONAL LOVE AND SUPPORT.

TABLE OF CONTENTS

LIST OF TABLES

LIST OF FIGURES

ACRONYMS

EBSD	Electron backscattered diffraction
EDS	Energy dispersive spectroscopy
SEM	Scanning electron microscopy
XRD	X-ray diffraction
LHV	Lower heating value

GREEK LETTERS

β-Mg	Beta Magnesium
α-Mg	Alpha Magnesium
γ-Mg	Gamma Magnesium
$K\alpha_1$	Main wavelength of XRD
$K\alpha_2$	Second wavelength of XRD
λ	Wavelength
Θ	Braggs angle
η	Lattice strain
μm	10^{-6} meter (micron)
ρ	Density of the balls

CHAPTER 1

INTRODUCTION

1.1 Why do we need hydrogen as a fuel?

There have been significant concerns about the rising levels of CO_2 due to the continuously increasing energy demands of the growing population. Increasing CO_2 levels have caused serious environmental issues such as global warming. The energy demand in 1973 was reported to be 6128 Mtoe (million tonnes of oil equivalent) which doubled over three decades to 11435 Mtoe in 2015. If this situation persists, the energy demand is expected to reach 17100 Mtoe by 2030 [1]. Due to limited amount of fossil fuels present in the earth's crust and the rising environmental concerns related to its usage, it is inevitable to find an alternative clean and sustainable source of energy.

Hydrogen can be used for power generation either by burning in an internal combustion engine or electrochemically used in a fuel cell. Either ways, the hydrogen reacts with oxygen to form water with a very minimal amount of NO_x (when reaction is carried out at very high temperatures).

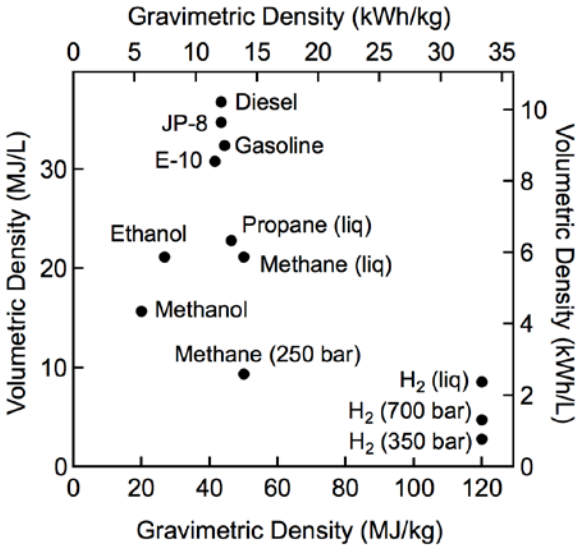

Figure 1.1 Comparison of specific energy and energy density for different fuels based on lower heating values [2]

Hydrogen also has about three times higher calorific value (120 MJ/Kg) as compared to petrol (43MJ/Kg). However, it can be seen clearly from Figure 1.1 that based on volumetric density, gasoline has a density of 32 MJ/L whereas liquid hydrogen has a density of only 8 MJ/L based on the lower heating values.

Therefore, it can be understood that hydrogen is a significantly cleaner source of energy when compared to the fossil fuels.

1.2 Challenges in Storing hydrogen

Even though hydrogen is a proven clean source of energy with great potential to replace the fossil fuels, it still cannot replace gasoline currently due to the major problem of its storage.

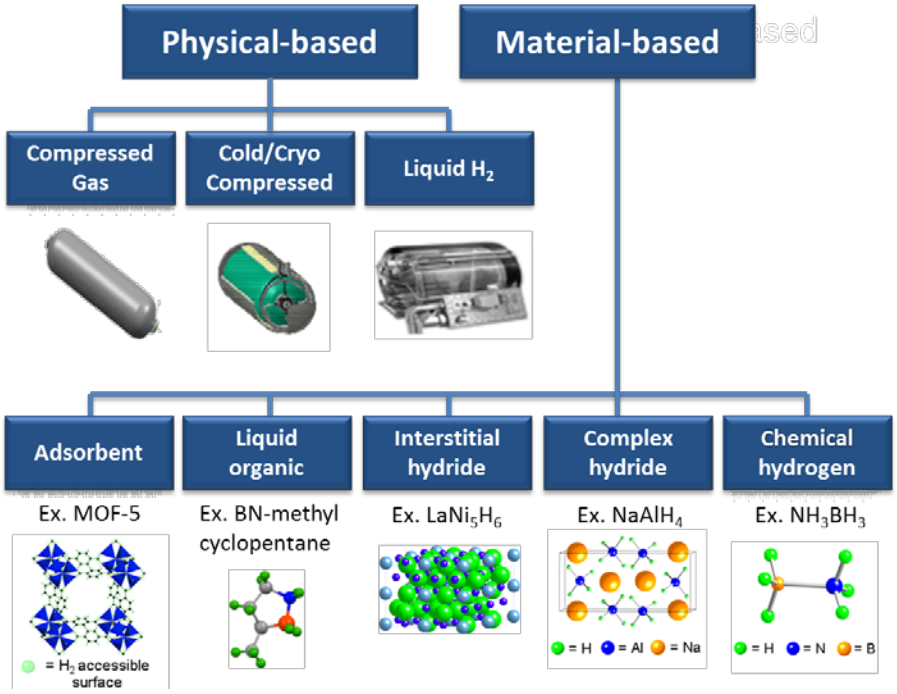

Figure 1.2 Different types of hydrogen storage methods and media [2].

Hydrogen storage can be categorized into two different forms: Physical based (hydrogen storage in gaseous and liquid form in high pressure cylinders) and material based (storage of hydrogen when physisorbed or chemisorbed by a material).

The material based storage of hydrogen is the most promising and mature technology. Material

based storage of hydrogen is a better alternative to physical based for numerous reasons.
The problems faced in storing hydrogen are described below:

1.2.1 Hydrogen storage in gaseous phase

This is the most common method of storing compressed hydrogen in cylindrical tanks. Presently, a working pressure of at most 700 bar can also be achieved using composite cylinders. Composite cylinders are lighter in weight than metal and comprise of an inner liner (made of Aluminum, steel or polymer) wound by carbon fibers and sealed in a polymer resin. At the maximum working pressure of 700 bar the gravimetric capacity was observed to be 4.5 wt%. However, the volumetric capacity was only 0.025 KgH_2l^{-1} [3]. Higher pressures will definitely improve the volumetric capacity but the energy needed for the compression at pressures more than 700 bar is 15% of the L.H.V. (lower heating value) of the stored hydrogen. Moreover, the cylindrical shape of the storage tanks is not the best shape when used in mobile applications since, it consumes a lot of space. There is also a significant safety concern related to this type of storage since there could be a leakage as the hydrogen stored is at very high pressures. Therefore, storing hydrogen in gaseous compressed form is not the most practical method of storing hydrogen especially in mobile applications.

1.2.2 Hydrogen storage in liquid phase

To store the hydrogen in a liquid phase, very low temperatures are needed to be maintained. Hydrogen has a critical temperature of 33K above which it acts as a non-condensable gas. At a pressure of 1 atm, hydrogen has a boiling point of 20K, which gives a liquid density of 0.0708 Kgl^{-1} and a volumetric capacity of 2.35 $Kwhl^{-1}$. It is crucial to maintain the temperature of the storage vessel below 20K to minimize any boil-off. However, boil-off can only be minimized and not eliminated completely due to heat conduction through cables and fixtures and convection through the environment. This type of system is highly undesirable for mobile applications as the system needs constant cooling and also there are safety issues if the vehicle is parked at a closed space for a longer time due to the hydrogen boil-off.

1.2.3 Material based hydrogen storage / Solid state hydrogen storage

The storage of hydrogen when bound to a solid material (through physisorption or chemisorption) is referred to as solid state hydrogen storage. Solid state hydrogen storage technology is the most promising method to store hydrogen efficiently. It is also low cost and robust [4]. This method of storing hydrogen theoretically stores more hydrogen per unit volume than the other methods [5]. Of all the different materials used for storing hydrogen, magnesium is by far the best from the standpoint of its hydrogen storage capacity per unit mass (7.6wt% theoretical). However, there are some drawbacks of using magnesium as a hydrogen storage material. Magnesium has slow reaction kinetics and requires high temperature and pressures for storing hydrogen. The United States, Department of Energy (D.O.E.) has set tough targets for the development of hydrogen vehicles. The D.O.E. targets for 2020 and ultimate targets are mentioned in the table below:

Table 1.1 Projected performance and Cost of Materials-Based Automotive Hydrogen storage 2020 and ultimate targets set by D.O.E. [2]

Storage system Targets	**Gravimetric Density (Kwh/Kg system)**	**Volumetric Density (Kwh/L system)**	**Cost ($/Kwh)**
2020	1.8	1.3	10
ultimate	2.5	2.3	8

Therefore, while developing an efficient hydrogen storage system the D.O.E. targets should always be kept in consideration.

A detailed description on solid state hydrogen storage has been provided in the next chapter.

1.3 Hypothesis of the research

Inspired by the studies above, the following idea came out. It is possible to develop an efficient Magnesium based hydrogen storage system by adding a catalyst (Nickel) and ball milling the magnesium particles to obtain better hydrogen storage characteristics.

1.4 Objectives of the thesis

The general objective of my research is to obtain the most suitable (highest and fastest hydrogen storage) parameters for the storage of hydrogen in the Magnesium-Nickel system. Therefore, the specific objectives are as follows:

Objective 1: To determine the most suitable composition of nickel (in weight %) with magnesium to achieve the highest hydrogen yield with fastest reaction kinetics.

Objective 2: To determine the milling time of magnesium-nickel powder to achieve the highest hydrogen yield with fastest reaction kinetics.

Objective 3: To propose the hydrogen charging pressure and temperature to achieve the highest hydrogen yield with fastest reaction kinetics.

Characterization of the samples was done to obtain phase distribution and morphology using X-ray diffractometry, scanning electron microscopy and energy dispersive spectroscopy for the analysis of elements.

CHAPTER 2

LITERATURE REVIEW

2.1 Introduction

Hydrogen can be bonded and stored in solid materials by numerous ways. Physisorbed hydrogen can be stored in Metal Organic Framework-5 (MOF-5), graphene and other carbonaceous materials. Hydrogen can also be stored in liquid organic form in compounds such as BN-methyl cyclopentane. Interstitial hydride and complex hydride such as $LaNi_5H_6$ and $NaAlH_4$ respectively can also be used to store hydrogen by the process of chemisorption. Chemisorption is a process where; the hydrogen atoms are chemically bonded with the host metal. This involves an electron transfer and higher bonding energy between the hydrogen atom and the host metal. Although there are several ways to store hydrogen in materials, there are some serious drawbacks associated to it such as cost, reaction kinetics etc. This chapter provides a detailed description of hydrogen storage in materials and the different effective methods to tackle the aforementioned drawbacks.

2.2 Physically bound hydrogen

Physisorption is a surface phenomenon where, hydrogen is bound at the surface of the materials by weak van der Waals interactions with an enthalpy of adsorption lying between (4 – 10 $KJmol^{-1}$). Due to this low enthalpy of adsorption very low temperatures (77 – 80K) are required for the adsorption process, so that the hydrogen molecules do not have too much thermal energy to overcome the weak interactions. Materials used for physisorption are those with high surface area. One method to increase the surface area is by increasing the porosity of the material. Important observations have been made in different porous materials such as high surface area carbon, Carbon Nano-tubes (CNTs), zeolites, Metal organic frameworks (MOFs) and polymers of intrinsic microporosity (PIMs). The Table 2.1 shows characteristics and properties of typical porous materials used for hydrogen storage.

Table 2.1 Characteristics and properties of typical porous hydrogen storage materials [6][7][8][9][10].

Material	Surface Area (m^2g^{-1})	Porosity (cm^3g^{-1})	Hydrogen storage capacity at 77K and 20 bar (wt %)
Porous carbon	3150	1.95	6.9
CNTs	1160	-	3.8[a]
Zeolites	670	-	2.2
MOFs	2200	0.89	6.1
PIMs	1050	0.40	2.7[b]

[a]Measured at 1 bar hydrogen.

[b]Measured at 15 bar hydrogen.

It can be clearly seen from the table 2.1 that most of the typical porous materials already meet the D.O.E. targets or are close to it. Porous materials have excellent cyclability as they do not undergo any changes during adsorption and desorption [4]. However, these materials do need cryogenic storage tanks for liquid hydrogen at 77K which is better than direct liquid state storage of hydrogen in tanks at (20K). Therefore, storing physisorbed hydrogen in porous materials has boil-off issues and since the physisorption process is exothermic, thermal management issues also arise during the adsorption process. All these reasons make physisorbed hydrogen unsuitable for mobile applications.

The problems associated with the physisorbed hydrogen can be overcome if the hydrogen is bounded to the material with a higher enthalpy for room temperature storage. This type of bonding can be achieved when the hydrogen is bonded to a metal which will be discussed later in this chapter.

2.3 Hydrogen storage in metal hydrides.

Metals have the capability of storing large amounts of hydrogen gas reversibly. The absorption of hydrogen in a metal hydride is a multi-step process described by the long-range attractive/short-range repulsive Lennard-Jones potential [11].

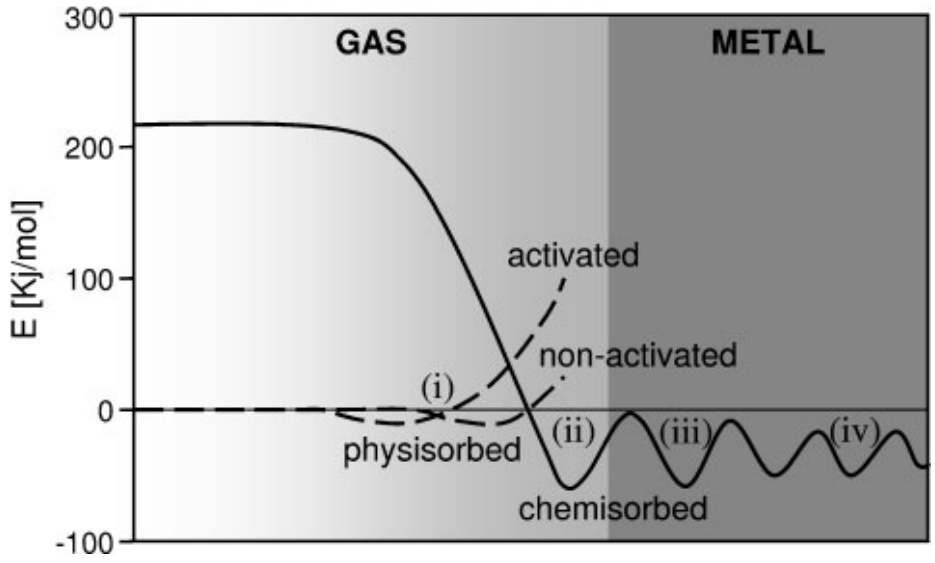

Figure 2.1 Potential energy curve for the Lennard-Jones potential for hydrogen binding to a metal indicating: (i) physisorption; (ii) dissociation and surface chemisorption; (iii) surface penetration and chemisorption on substrate sites; and (iv) diffusion [12].

As the molecular hydrogen approaches the metal surface successive minima of the potential is observed from the figure 2.1. Molecular hydrogen is first physisorbed on the surface of the metal by weak van der Waals forces. If pressure and temperature are increased the physisorbed hydrogen is then dissociated into the metal and becomes chemisorbed. In chemisorption, a chemical bond is developed between hydrogen and the corresponding metal with a decent binding energy (above 50KJ mol^{-1}) [11]. After the chemisorption, the hydrogen molecules move to the subsurface sites and diffuse through the material. This state is referred to as the α-phase.

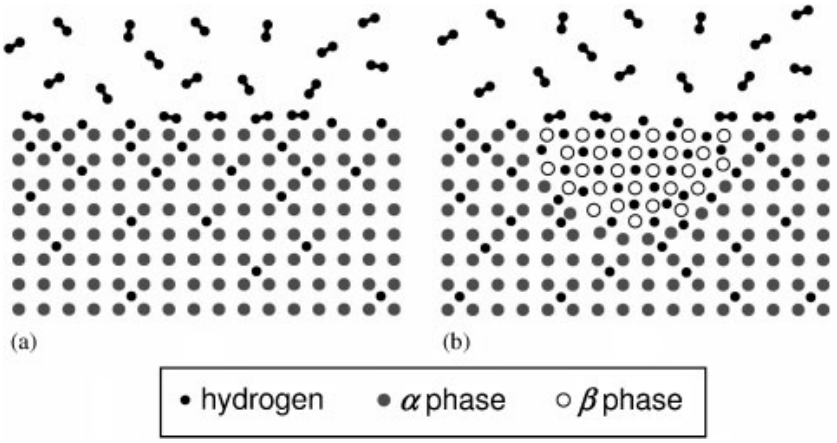

Figure 2.2 Formation of the β-phase from α-phase in a metal hydride [11].

As the hydrogen molecule concentration increases in the α-phase, hydrogen-hydrogen interactions become more prominent and a more stable phase forms known as the β-phase as shown in the Figure 2.2. This formation of the β-phase causes the crystalline structure of the metal to change, volume to expand and creates a nucleation energy barrier.

Metal hydrogen bond is a strong bond and provides with a high density of hydrogen molecules trapped in the host metal at a moderate pressure.

The Figure 2.3 shows the volumetric and gravimetric capacity of different hydrogen storage media.

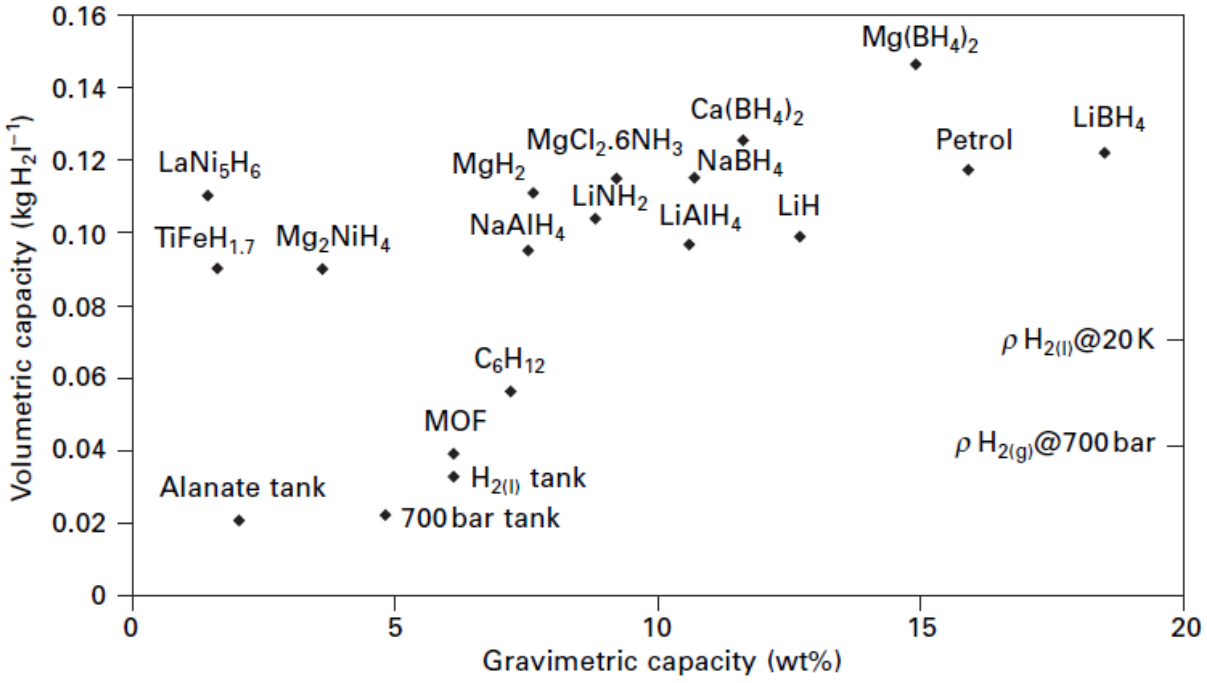

Figure 2.3 Hydrogen storage capacities for a range of storage media [4].

The volumetric capacity of most of the materials is superior to that of liquid hydrogen. Most of the materials shown in the Figure 2.3 clearly do not meet the D.O.E. targets and the ones that do meet the targets require high dehydrogenation enthalpy. Destabilization can help lower the dehydrogenation temperature since $T = \Delta H/\Delta S$ therefore, lower temperature could be obtained by increasing the entropy. To destabilize a hydride, destabilizing agent (catalyst) is added.

2.4 Magnesium as a hydrogen storage medium.

Magnesium has been the material of most interests among scientists due to its high reactivity, low cost, low density and a high theoretical hydrogen storage capacity of 7.6 wt%.

Upon hydrogenation, the hydrogen atoms are introduced into the hexagonally close-packed (HCP) magnesium metal lattice. The hydrogen atoms first occupy the tetrahedral interstitial sites forming the α-phase with up to 9at% concentrations of hydrogen at 650°C [13]. Further addition of hydrogen leads to the formation of the β-phase which has a tetragonal lattice structure with lattice parameters a = 0.452nm and c = 0.302nm and density = 1.42×10^3 kgm^{-3} [14]. However, pure magnesium is prone to oxidation and has slow hydriding and dehydriding rates and high hydrogen dissociation temperatures (above 290°C) at 1 bar [15].

To improve the hydrogen storage characteristics different techniques have been used: the most common techniques are ball milling and adding a catalyst.

2.4.1 *Ball milling to improve the hydrogen storage characteristics.*

Ball-milling is one of the most common approach to improve the hydrogen storage characteristics of metal hydrides. Ball mills are of different types ranging from vibratory to planetary-style mill. Different styles of ball milling have different energies and temperatures subjected to the material being milled. A planetary ball-mill can reach at temperatures above 500K [16][17].

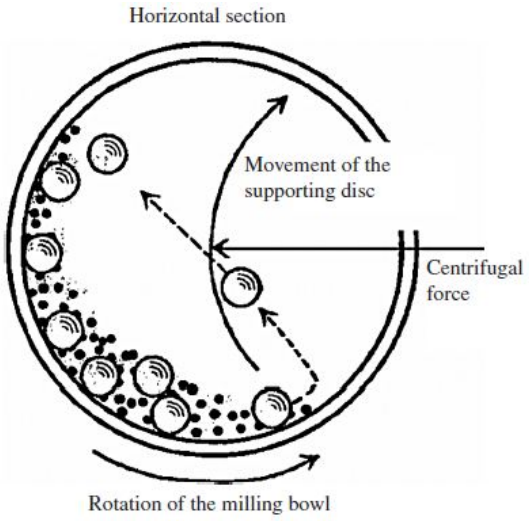

Figure 2.4 Schematic view of motion of the ball and powder mixture in a ball mill [18].

In a ball mill, the material placed in the ball milling container is subjected to high energy collisions from the balls. The ball milling system has one turn disc on which ball milling containers are placed. The milling containers and the turn disc rotate in opposite direction creating a movement of the balls as shown in figure 2.4.

Magnesium ball milled with 35wt% of amorphous transition metal alloys, where a 3.4wt% hydrogen release was observed at 300°C in 30 mins compared to pure magnesium with no ball milling released the same hydrogen in 75 mins [19]. This is because upon ball milling the particle size of the material is reduced and surface roughness is increased. Also, during ball milling defects are introduced in the material, nucleation sites are increased and the diffusion path length for hydrogen leaving the hydride is reduced. It was also seen that ball milling reduced the desorption time of pure magnesium to 10 mins at 623K from 70 mins at the same temperature [20].

2.4.2 Addition of catalyst to improve the hydrogen storage characteristics.

Addition of a catalyst that reacts with the magnesium to form an intermediate state is helpful in reducing the heat of formation. An example of this is Mg doped with 5% Silicon, resulting in the reduction of the enthalpy of formation to 40 kJ/mol [21]. Catalysts can also help improve the resistance to contaminants by allowing a reduced activation barrier route through an oxide layer [4].

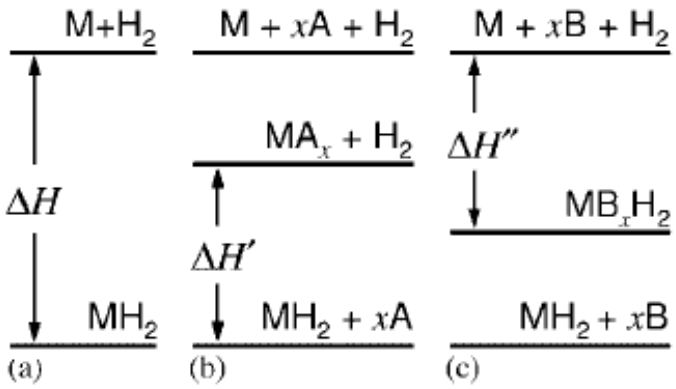

Figure 2.5 Different ways of reducing the enthalpy of formation by the addition of a catalyst [11].

As seen in figure 2.5 the enthalpy of formation in a hydriding process can be reduced by the introduction of a catalyst in different ways:

(a) The heat release between the initial and final product is given by ΔH.
(b) The compound A when added forms a metastable state with the host metal thereby, reducing the enthalpy to ΔH'.
(c) In this case the addition of the catalyst creates a destabilized hydrogenated state and hence the enthalpy of formation is reduced.

The hydrogen absorption and desorption characteristics can be significantly improved by combining ball milling and catalyst addition through a technique known as spillover in which the hydrogen molecules dissociate on the catalyst surface [22]. Lesser quantity of catalyst is needed when used along with the ball milling process as it gets dispersed at the nano-scale throughout. By adding upto 1 wt% of Palladium to MgH_2 and ball milling, dispersed nanoparticles of Pd were observed over the magnesium hydride surface [23][24][25][26][27]. The sample absorbed 6wt% of hydrogen and both hydrogen absorption and desorption rates were improved from 120 mins (for the same particle size with no Pd) to 40 mins [25]. Addition of other transition metals such as Cobalt [28], Titanium [29], Iron [28], Vanadium [29][30][20][31] and Nickel [28] have been studied. Mg ball milled with 10 wt% of CeO_2 was reported to absorb 3.43 wt% of hydrogen at 300°C and 20bars of hydrogen pressure in only 5 minutes [32]. Mg-10wt%Fe_2O_3 ball milled was observed to absorb upto 5.5 wt% of hydrogen at 320°C and 12 bar of hydrogen pressure. However, the desorption was significantly slow (60 minutes) [33]. A desorption time of 33 minutes was

reported with MgH_2-5wt%V ball milled and hydrided at 200°C and 10 bar of pressure with a hydrogen storage capacity of 5.8 wt% of hydrogen stored [31]. Nickel has been reported to significantly improve the catalytic activity in the hydriding and dehydriding process [34]. Moreover, nickel is also cheap when compared to most of the transition metals. Ball milled Mg_2Ni hydrided at 7 bar of hydrogen pressure absorbed 3.4 wt% of hydrogen with a half reaction time of just 1 minute [35]. Mg_2Ni is stable only at temperatures above 250°C and upon cooling becomes a low temperature Mg_2Ni phase [36]. When heated to a temperature above 250°C Mg_2NiH_4 is formed with a cubic symmetry and a = 0.6490nm [37]. When mixed with 1 wt% Pd and ball milled, MgH2 was reported to absorb 2.5 wt% of hydrogen at 200°C and15 bar of pressure in 27 minutes [36]. One major drawback is that Mg_2Ni has a theoretical maximum hydrogen capacity of 3.6 wt% only. Hence, it is desirable to reduce the nickel concentration to the minimum to obtain the desired results. There are numerous publications on the enhancement of the hydrogen storage properties by using ball milling and adding a transition metal. Many experiments have reported: Mg_2Ni ball milled and hydrided at 300°C at a hydrogen pressure (1-29 bar) stored 3.2-4.1 wt% of hydrogen [38][39][36][40][41][42]. It is clearly understood that even though Magnesium and various transition metal systems have been thoroughly studied, not much research has been done on Mg-Ni system alone by varying the parameters such as hydriding/dehydriding pressure and temperature, ball milling time etc.

CHAPTER 3

MATERIALS AND METHODOLOGY

This chapter provides a detailed summary of the materials and the experimental techniques used to achieve the desired objectives. It also covers certain problems that were faced during these experiments.

3.1 Materials

The materials used in this project were:

Mg powder 98% purity, reagent grade (MFCD00085308) 20-230 mesh by Sigma Aldrich.

Nickel powder 99.95% purity (MFCD00011137) APS 2.2-3.0 micron by Alfa Aesar.

Stearic Acid 97% purity (AC17449-0010) by Fischer Scientific.

3.2 Methodology

The different experimental/analyses techniques used in this research work are described below.

3.2.1 Ball milling

Mg powder, Nickel powder and 3 wt% of Stearic acid were ball milled in a planetary ball milling machine (Torrey Hills- ND2L) with stainless steel cups (285ml) and balls (28 balls of 16mm and 6 of 18mm diameter) in an Argon atmosphere. Ball to powder ratio was 30:1 and milling speed was maintained at 400 RPM. Stearic acid was added in this process to avoid the cold welding of the magnesium powder and was kept to a minimum quantity.

Samples were produced in two different batches by varying the milling time and the nickel content. The following samples were produced

Table 3.1 Samples prepared for the experiments

Sample Number	Nickel (wt%)	Milling time (hours)	Pressure (bar)	Temperature (Celsius)
1	0	10	20	300
2	1	10	20	300
3	5	10	20	300
4	7	10	20	300
5	10	10	20	300
6	15	10	20	300
7	10	5	20	300
8	10	7	20	300
9	10	15	20	300
10	10	20	20	300
11	10	10	5	300
12	10	10	15	300
13	10	10	25	300
14	10	10	20	250
15	10	10	20	350

Since, there were too many samples and parameters to analyze the entire research work was divided into a series of steps.

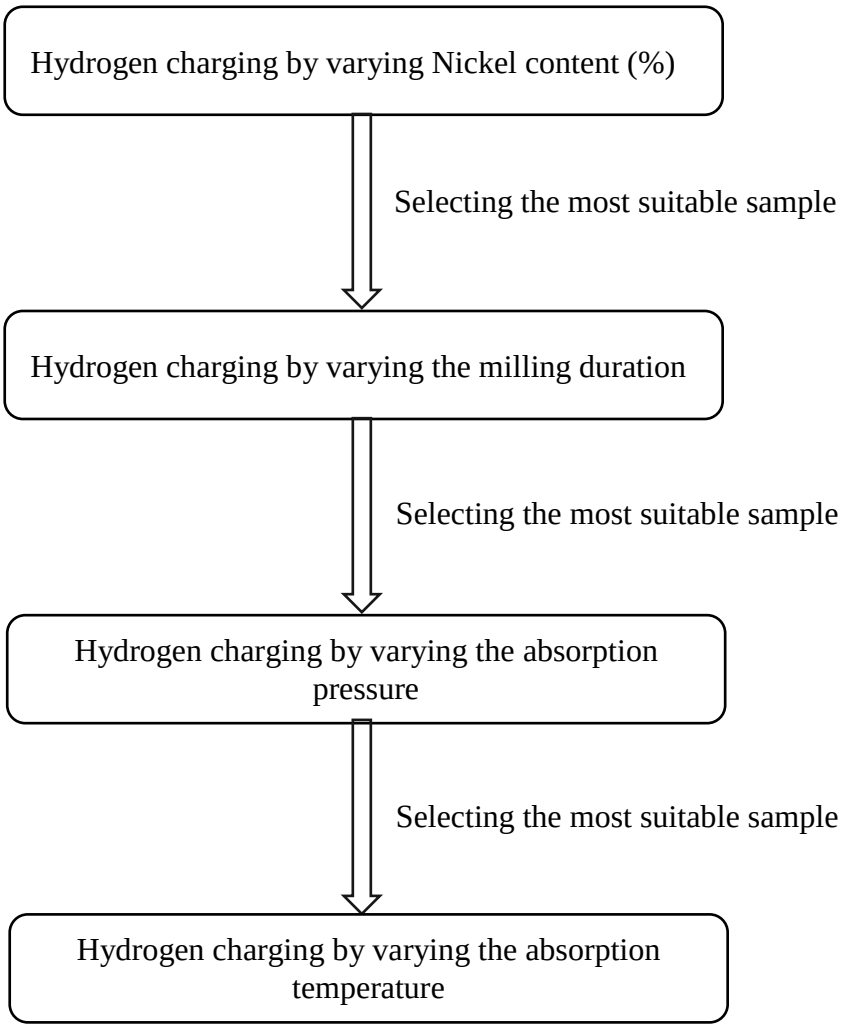

Figure 4.1. Chart showing the entire research work in a series of steps.

3.2.2 Hydrogen charging and discharging

The hydrogen charging and discharging processes were carried out in a laboratory made apparatus.

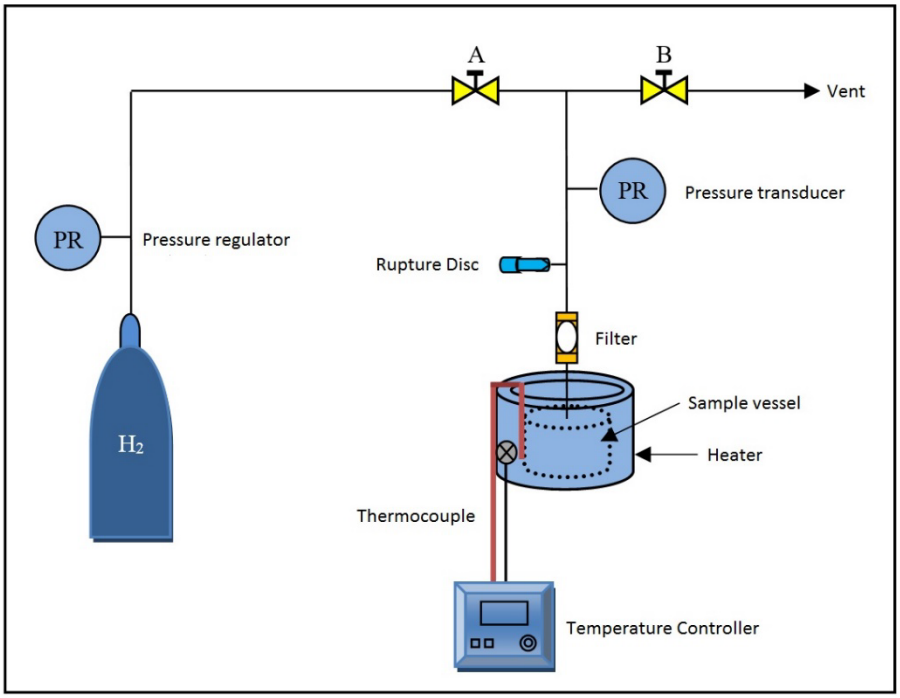

Figure 3.1. Laboratory-made apparatus for the hydrogen charging process [43].

As seen from the Figure 3.1, the hydrogen apparatus is mainly equipped with a hydrogen cylinder (HY 5.0UH-T, Ultra high purity grade 99.999%, Praxair), a pressure regulator (KPP1RSH422P2A030, Swagelok), a sample vessel (250 ml, 453HC-316-0719842151, Parr instrument), a rupture disc (Parr instrument), a heater (854HC, Parr instrument), a temperature controller (50°C to 1200°C, 210/TIMER-K model, J-KEM Scientific) with a ceramic insulated thermocouple (870°C, XC-20-K-24, Omega), a filter (pore size of 0.5 µm, SS-4FW-VCR-2), a pressure transducer (TE Connectivity measurements specialities M3021-000005-01KPG, operating pressure of 1000 PSI, maximum pressure of 2000 PSI, accuracy of ±1% and operating temperature of -20°C ~ 85°C) and a temperature sensor board (Phidgets 1048_0, ambient temperature max error of ±0.5°C, thermocouple max error of ±2°C and thermocouple temperature resolution of 0.04°C). The pressure transducer and temperature sensor board are connected to a computer running a program made in LabVIEW. All tubes (SS-T2-S-028-20), valves (SG-4UG-V51-VS), connectors and fitings (gasket, 457HC2) are purchased from Swagelok. Due to the high

operating pressure and risk of corrosion, all reactors, valves, connectors and fitting are made of 316 stainless steel. All valves are bellow sealed with maximum working temperature of 350°C and 240 bar, respectively.

Each discharging process was carried out in the homemade apparatus at atmospheric pressure and a temperature of 350°C. The amount of hydrogen discharged was measured in ml/min using a flowmeter (Agilent Technologies ADM 2000) connected to the vent. Hydrogen in the reaction system was assumed to behave as an ideal gas and the weight percentage of hydrogen was calculated using the ideal gas equation.

$$PV = nRT \quad (3.1)$$

Where, P = absolute pressure (atmospheric pressure in this case)

V = volume of the sample vessel (mL)

T = absolute temperature (K)

n = number of moles of hydrogen

R = universal gas constant (8.3145 J/mol K)

An overall accuracy in the hydrogen mass changes was ±5.4%. Leakage test on the apparatus was done at room temperature and 100 bar pressure for 12 hours. Before every charging process, degassing was done (3-4 times) to remove any unwanted gas or contaminants from the apparatus.

3.2.3 X-ray Analyses of powders

Microstructures of the powder samples was characterized by a Bruker D8 Discovery X-ray diffractometer with a chromium target.

$K\alpha_2$ stripping was done using the Rachinger method [44], considering $K\alpha_1 = 2.289760$ and $K\alpha_2 = 2.293663$. It was assumed that the $K\alpha_1$ and $K\alpha_2$ line profiles are identical in shape and not necessarily symmetrical, and the α_2 peak is half the intensity of the α_1 peak, and is shifted from it towards larger angles by

$$\Delta 2\theta = 2tan\theta(\Delta\lambda / \lambda) \quad (3.2)$$

Where, $\Delta\lambda$ is the dispersion separation $\lambda(\alpha_2) - \lambda(\alpha_1)$ in angstroms.

To convert the powder diffraction pattern into a simpler profile, Pseudo-Voigt profile fitting was performed using the software EVA V2. This software was used to determine the different phases of magnesium, nickel and hydrogen present in the samples.

3.2.4 Scanning electron microscopy/Energy dispersive spectroscopy

Morphology of the samples and the elemental distribution chart was studied using a Hitachi SU6600 Scanning electron microscope. AZTEC 2.0 data acquisition software was used to acquire the electron diffraction patterns. EDS makes use of the X-ray spectrum emitted by a solid sample bombarded with a focused beam of electrons to obtain a localized chemical analysis. All elements from atomic number 4 (Be) to 92 (U) can be detected in principle, though not all instruments are equipped for 'light' elements ($Z < 10$). Qualitative analysis involves the identification of the lines in the spectrum and is straightforward owing to the simplicity of X-ray spectra. Quantitative analysis (determination of the concentrations of the elements present) entails measuring line intensities for each element in the sample and for the same elements in calibration Standards of known composition. By scanning the beam in a television-like raster and displaying the intensity of a selected X-ray line, element distribution images or 'maps' can be produced. Also, images produced by electrons collected from the sample reveal surface topography or mean atomic number differences according to the mode selected. The scanning electron microscope (SEM), which is closely related to the electron probe, is designed primarily for producing electron images, but can also be used for element mapping, and even point analysis, if an X-ray spectrometer is added. There is thus a considerable overlap in the functions of these instruments [45]. The raw EDS data was analyzed using Oxford Instruments Channel 5 processing software. The average particle size was calculated using the SEM image and the software ImageJ.

CHAPTER 4

RESULTS AND DISCUSSION

This chapter gives a detailed description of the results obtained and the conclusions drawn from them. Since, there were too many samples and parameters to analyze the entire research work was divided into a series of steps.

4.1 Effect of varying Nickel composition on the hydrogen storage characteristics of magnesium-nickel alloy.

A batch of samples having different compositions of nickel were prepared as discussed in the chapter 3. These samples were charged with hydrogen at a constant hydrogen pressure of 20 bar at 300°C for an hour.

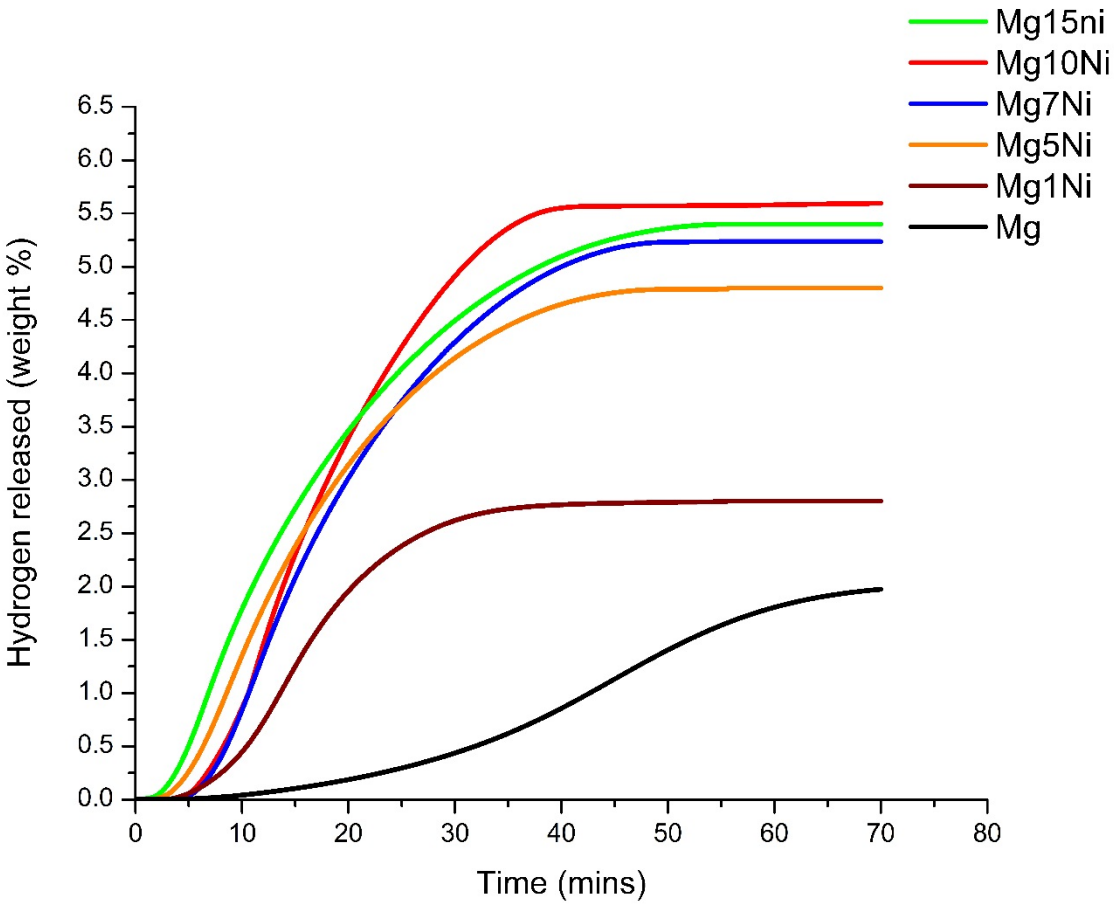

Figure 4.2. Effect of varying Nickel content on the hydrogen storage capacity of ball milled Magnesium-Nickel alloy.

Figure 4.2 shows the effect of changing the nickel content in the various ball milled samples. All the samples were ball milled for 10 hours and the nickel content was varied (1wt%, 5wt%, 7wt%, 10wt% and 15 wt%). It can be clearly seen that pure magnesium even after ball milling has very slow reaction kinetics when compared to the other samples containing nickel. It can also be seen

that Mg10wt%Ni shows the highest hydrogen storage capacity (≈ 5.6wt%) with the fastest kinetics. Further or lesser amount of nickel addition in the sample has resulted in a lower hydrogen storage capacity. This is because nickel is a catalyst and the main metal for absorbing hydrogen is magnesium. Adding more wt% of Ni reduces the overall content of Mg and adding lesser wt% of nickel makes the catalyzing process ineffective.

Therefore, it is essential to keep the nickel quantity to the minimum without compromising to its benefits [34].

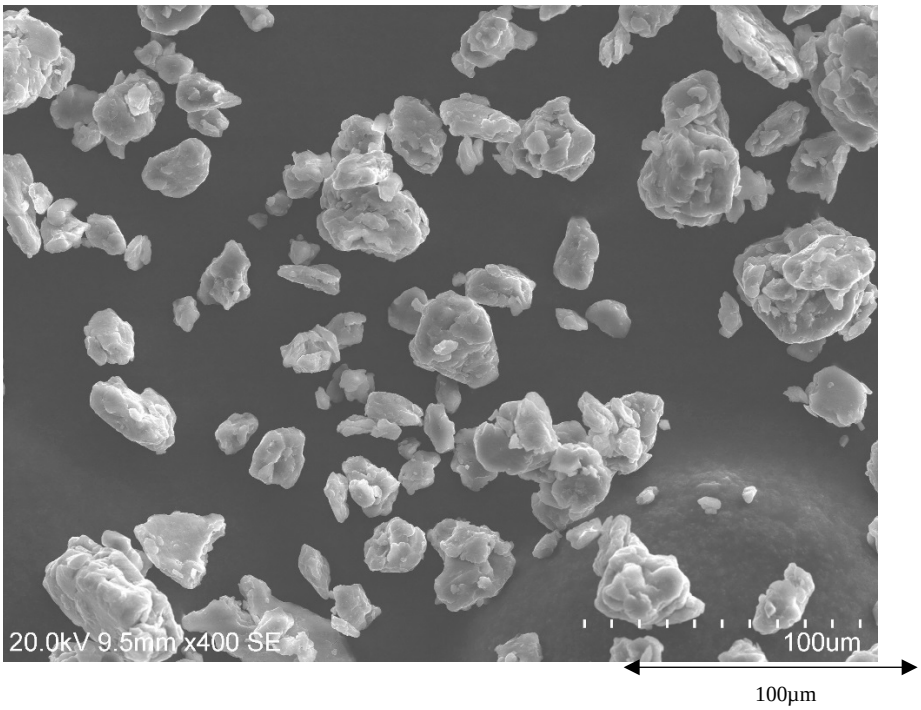

Figure 4.3. SEM image of Mg-1wt%Ni ball milled for 10 hours.

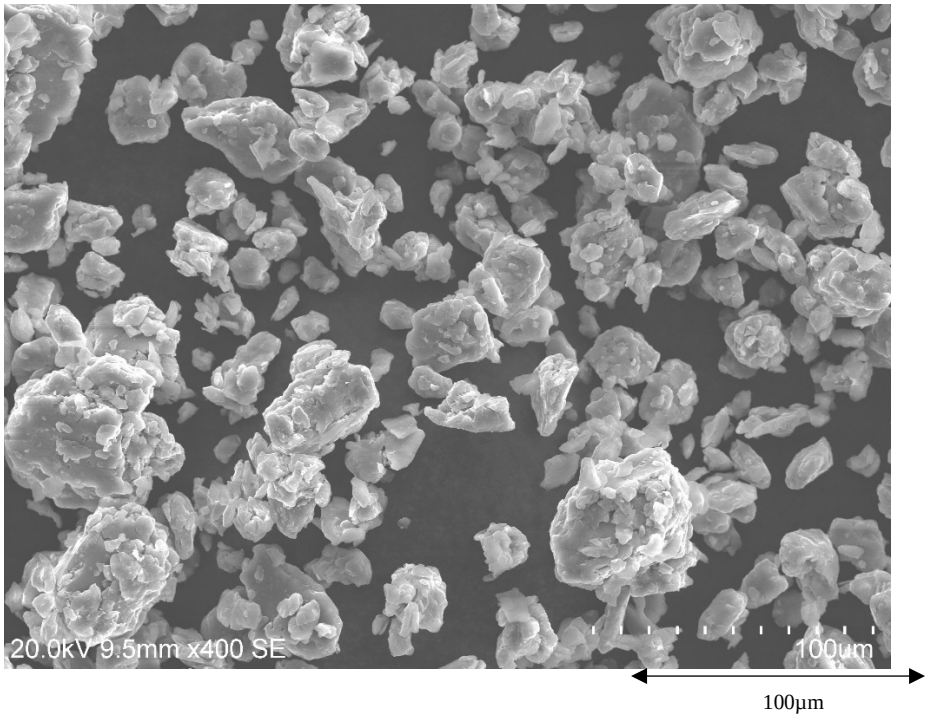

Figure 4.4. SEM image of Mg-5wt%Ni ball milled for 10 hours.

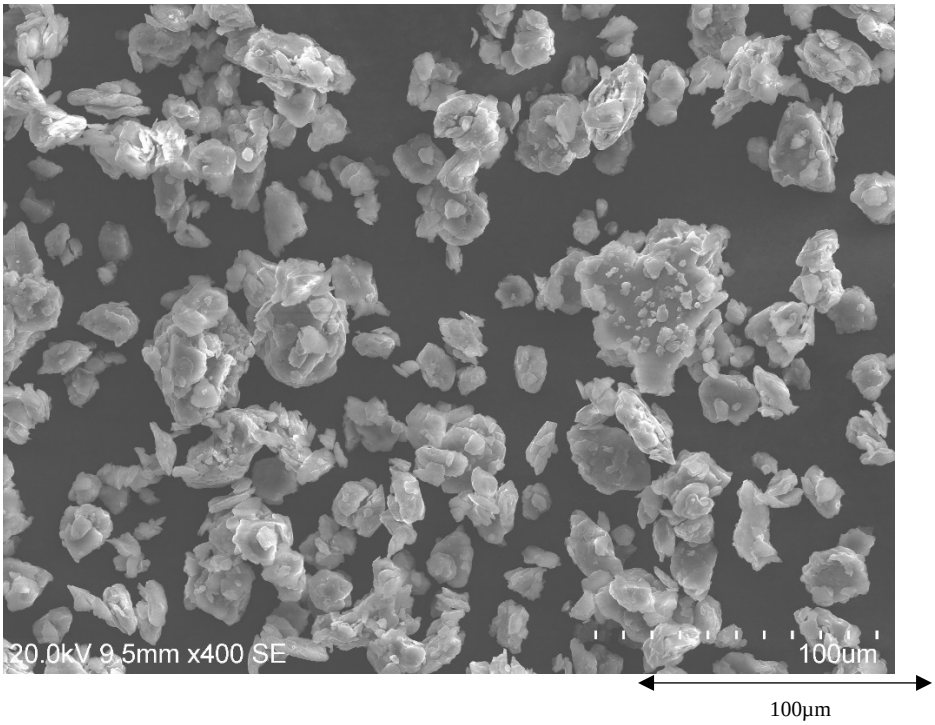

Figure 4.5. SEM image of Mg-7wt%Ni ball milled for 10 hours.

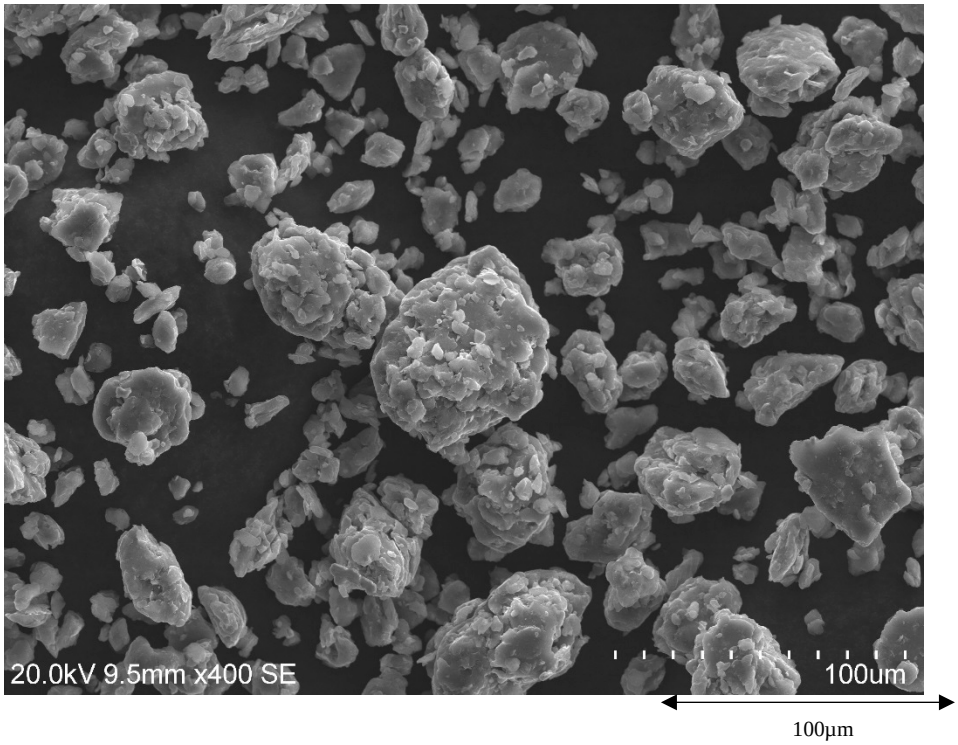

Figure 4.6. SEM image of Mg-10wt%Ni ball milled for 10 hours.

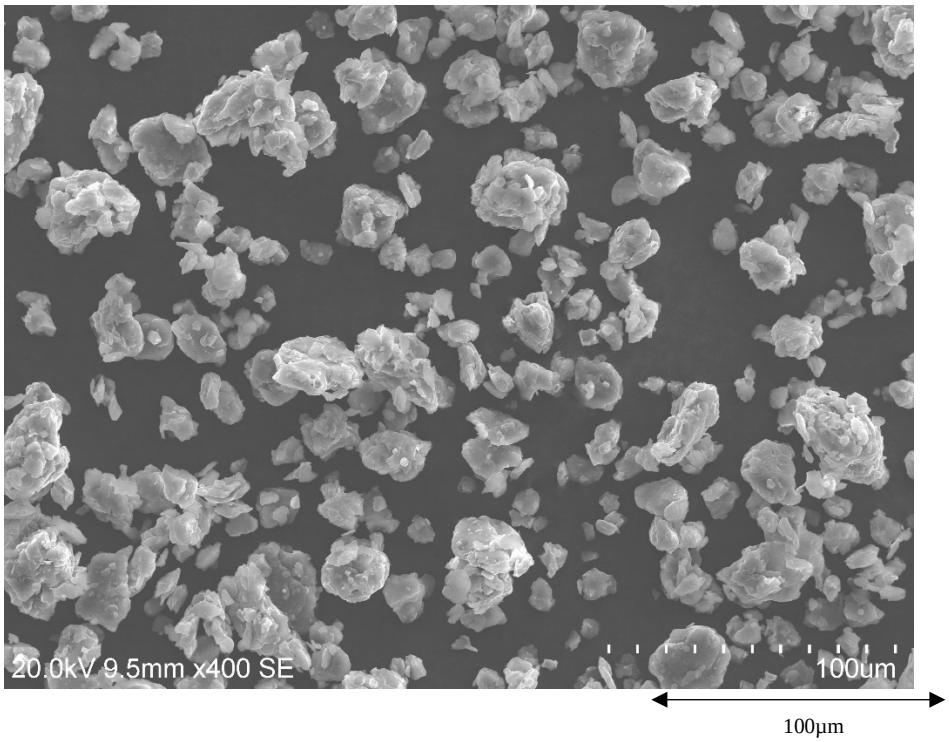

Figure 4.7. SEM image of Mg-15wt%Ni ball milled for 10 hours.

Figure 4.3, 4.4, 4.5, 4.6 and 4.7 show the SEM images of magnesium ball milled for 10 hours with 1%, 5%, 7%, 10% and 15% Nickel respectively.

The SEM images reveal that the samples milled with different compositions of nickel for 10 hours have a laminated structure with layers of flattened magnesium and nickel particles. Mg-1wt%Ni has the least number of layers amongst all the samples. This could be due to the lesser quantity of nickel present in Mg-1wt%Ni. Mg-Mg particles are much easily cold welded when compared to Mg-Ni particles. Therefore, the Mg-1wt%Ni particles are also observed to have the most homogenous and refined structure when compared to the other samples with different quantity of nickel present.

As the amount of nickel present in the sample is increased, a more laminated and layered structure is observed, facilitating more effective surface area for the hydrogen atoms to bond.

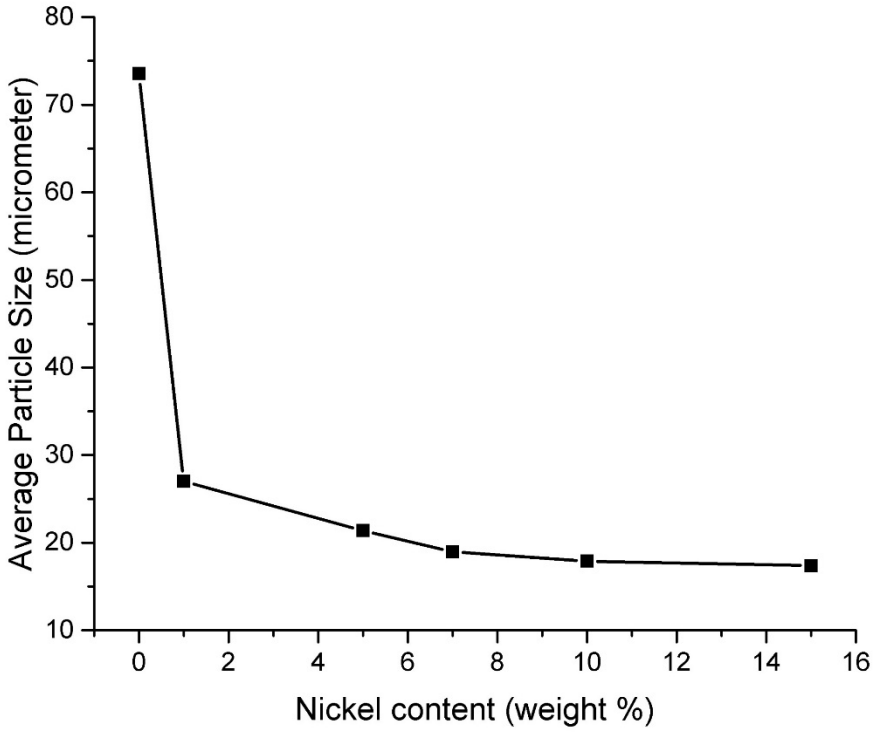

Figure 4.8. Variation of average particle size by changing the nickel composition.

The particle size was observed to decrease with the addition of nickel to the magnesium powder. The ball milling process comprises of two different sub processes: Fracturing and cold welding,

which occur simultaneously. From the observed results, it can be said that with the increase in the amount of nickel, the cold welding is reduced or the fracturing is increased.

4.2 Effect of varying ball milling time on the hydrogen storage characteristics of magnesium-nickel alloy.

Since Mg-10wt%Ni was selected as the best sample when varying different nickel compositions, another batch of samples was produced by ball milling the Mg-10wt%Ni for different durations (5, 7, 10, 15 and 20 hours). These samples were again charged at a hydrogen pressure of 20 bar and a temperature of 300°C. Discharging was done at 350°C and atmospheric pressure using a flowmeter.

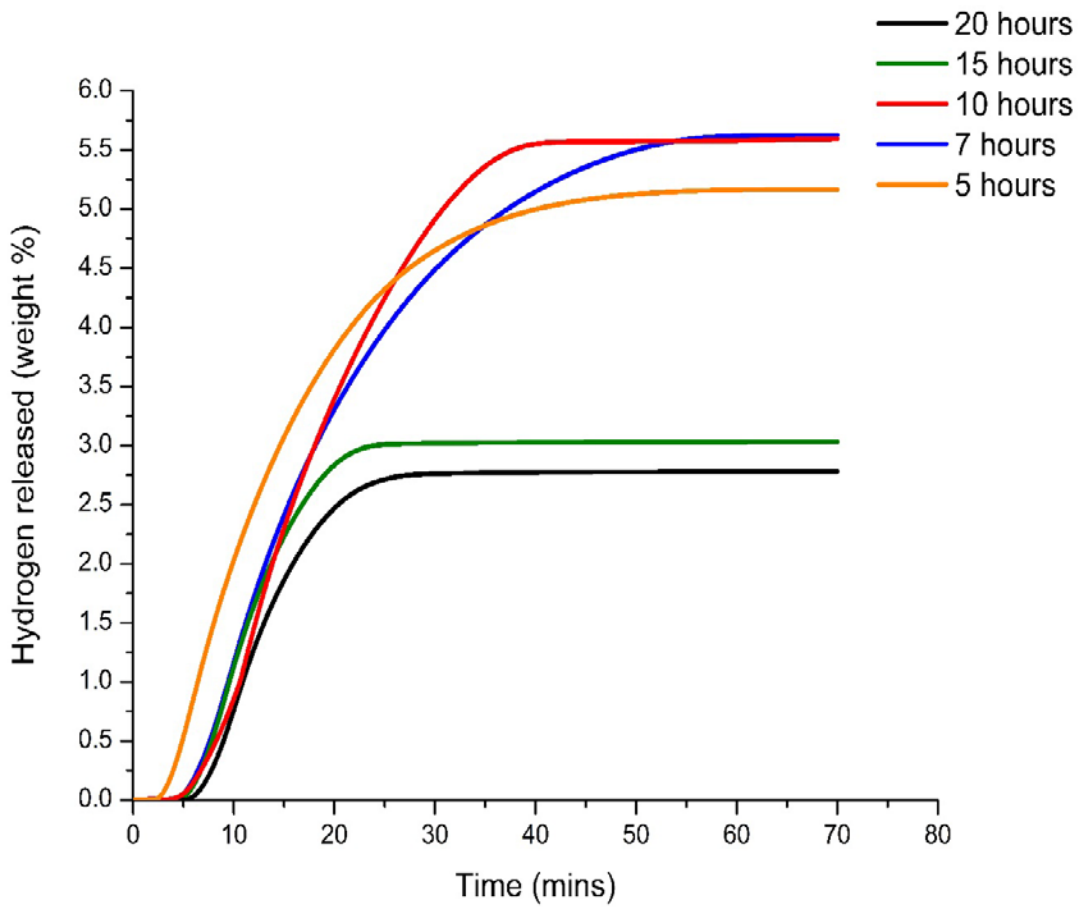

Figure 4.9. Effect of varying ball milling time on the hydrogen storage capacity of Magnesium-10wt%Nickel.

It can be clearly seen that there is a very minimal difference between the storage capacities of the sample milled for 7 hours (≈5.7wt%) and 10 hours (≈5.6wt%). However, the discharging rate of the sample milled for 10 hours is substantially higher as compared to the sample milled for 7 hours. A higher duration of ball milling (15 and 20 hours) resulted in a reduced hydrogen storage capacity.

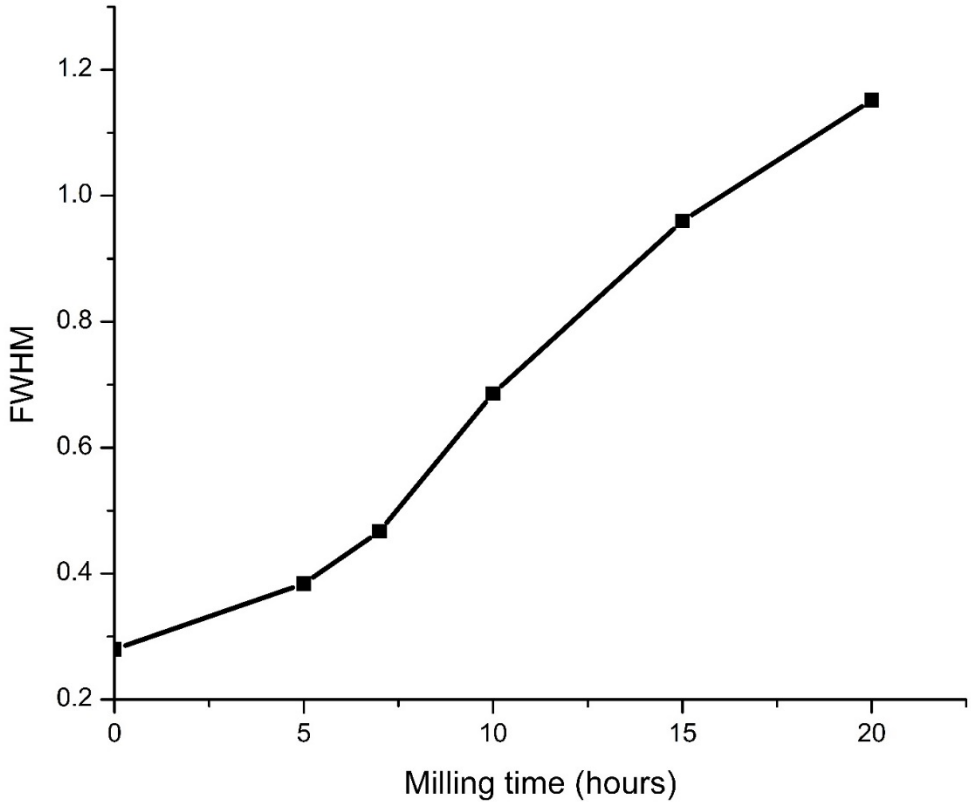

Figure 4.10. Effect of varying ball milling time on the full width at half maxima.

This reduction in the hydrogen storage capacity is attributed to the excess strain in the nanocrystals and the induced disorder reducing the total number of binding sites for the hydrogen [11] which can be clearly seen form the Fig 4.10. Lesser ball milling time of 5 hours has also shown a reduction in the hydrogen storage capacity.

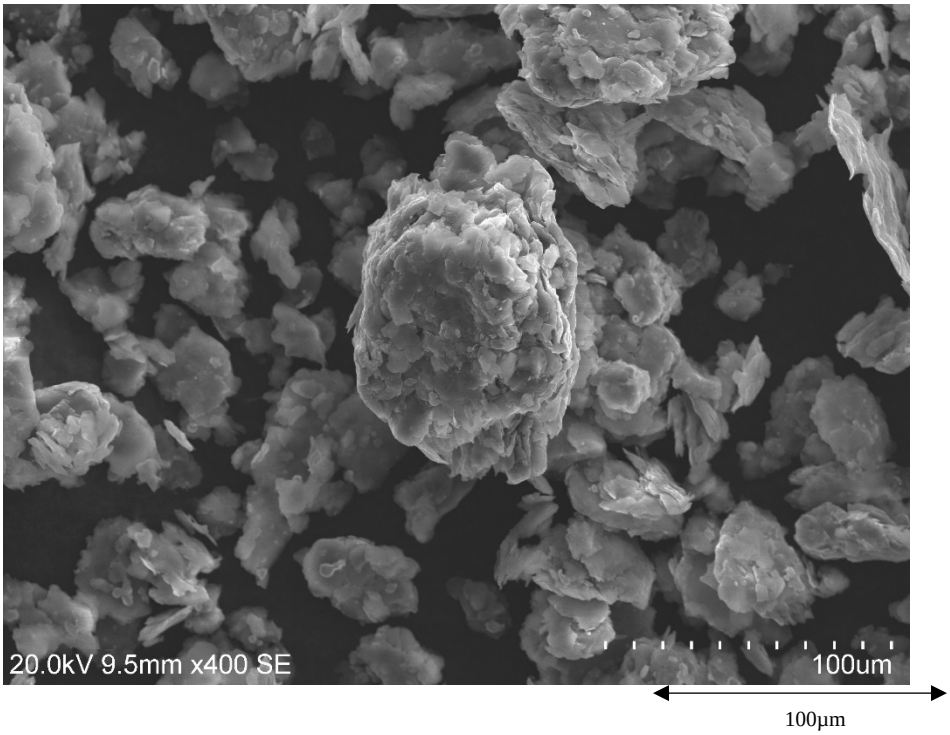

Figure 4.11. SEM image of Mg-10wt%Ni ball milled for 5 hours.

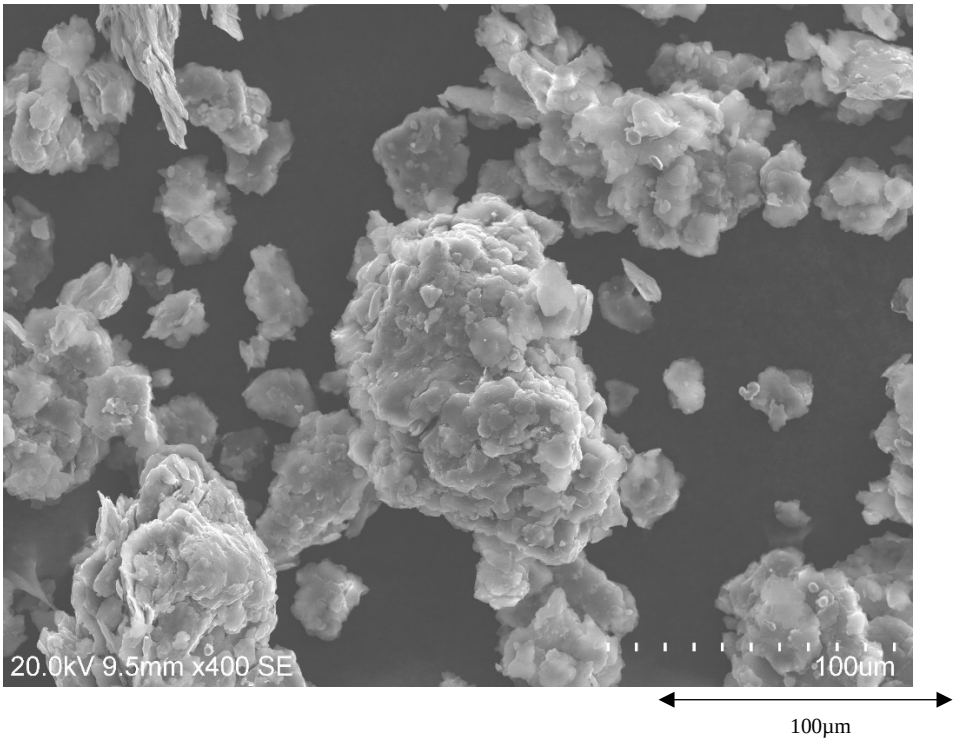

Figure 4.12. SEM image of Mg-10wt%Ni ball milled for 7 hours.

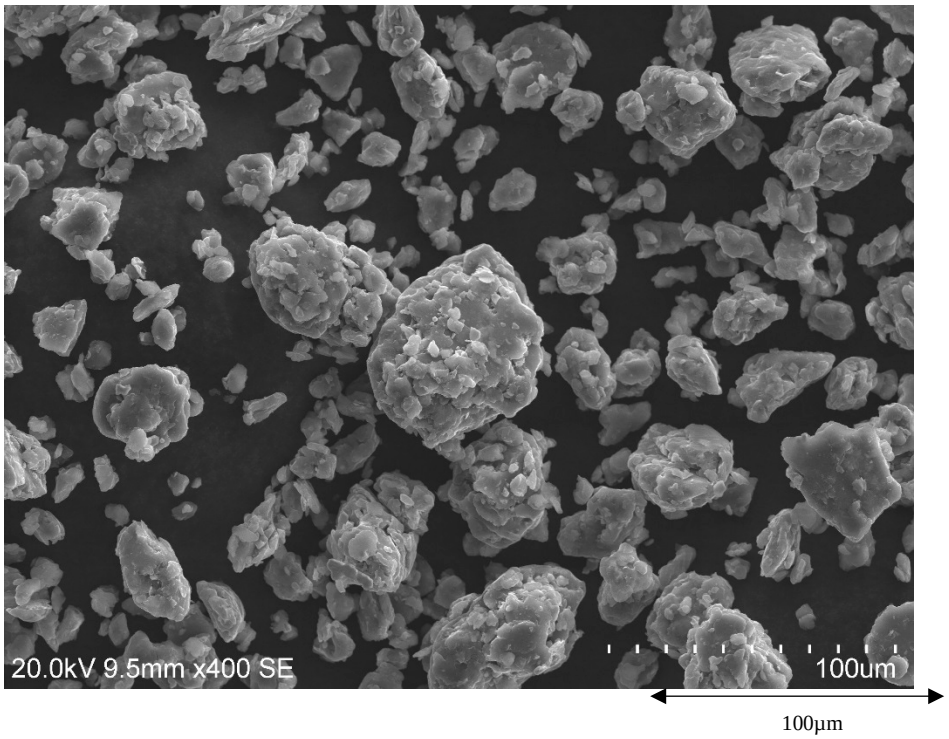

Figure 4.13. SEM image of Mg-10wt%Ni ball milled for 10 hours.

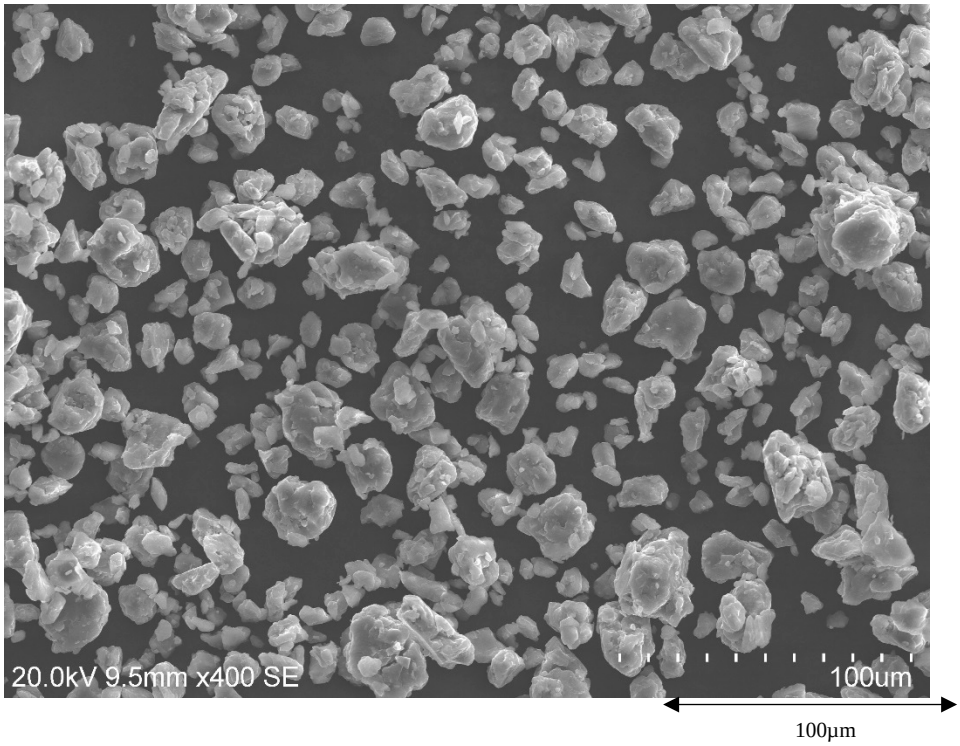

Figure 4.14. SEM image of Mg-10wt%Ni ball milled for 15 hours.

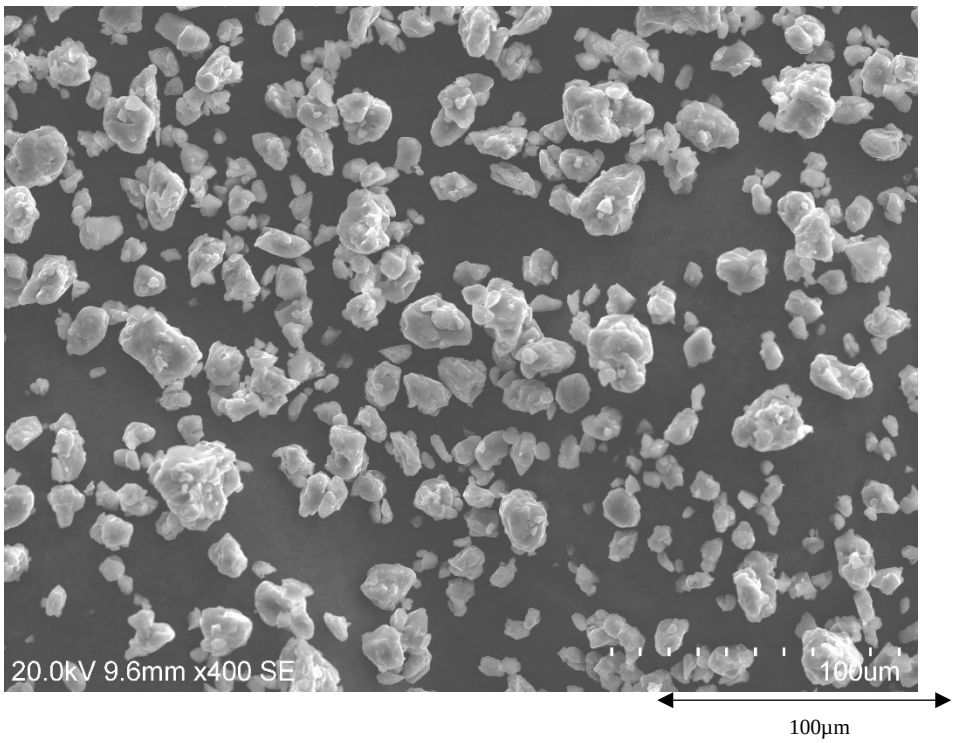

Figure 4.15. SEM image of Mg-10wt%Ni ball milled for 20 hours.

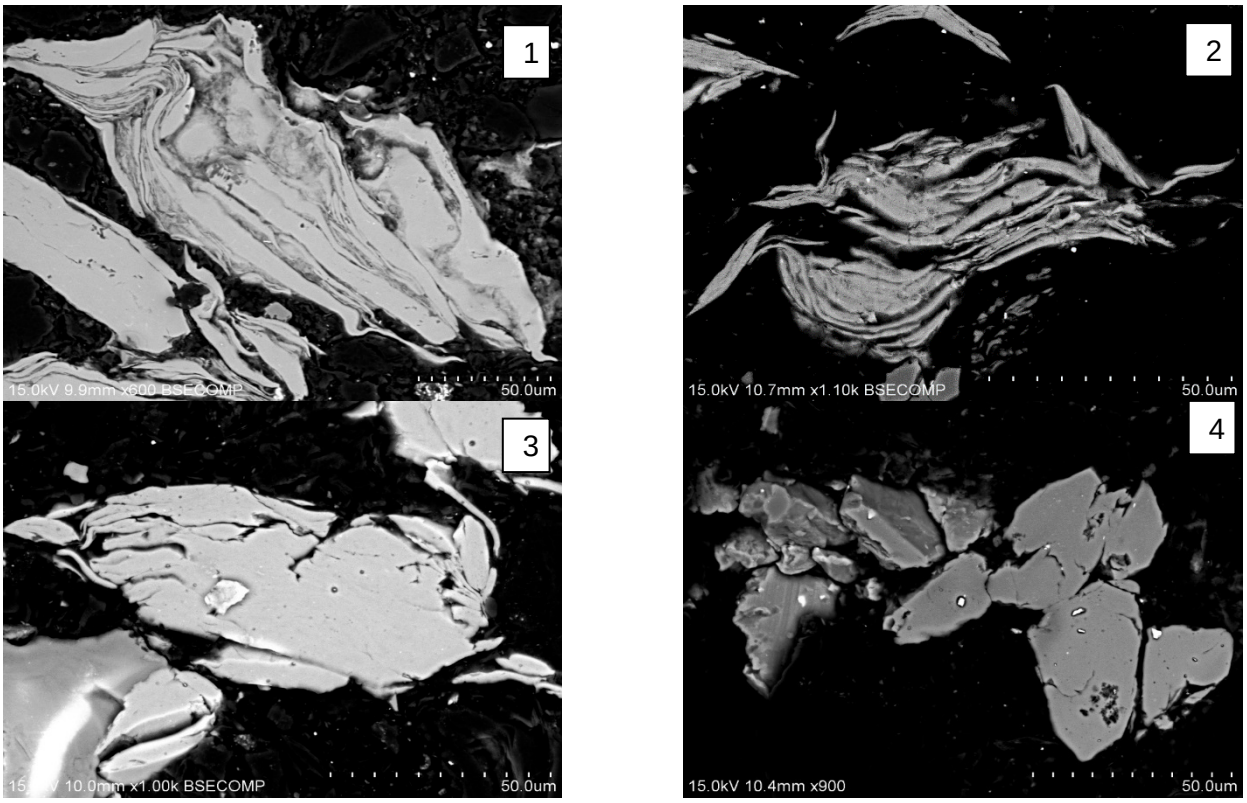

Figure 4.16. Cross-sectional SEM image of Mg-10wt%Ni ball milled for 5, 10, 15 and 20 hours.

The particles, after milling for 5 hours are formed by the cold welding of a few flattened particles producing a laminated structure with many layers. The microstructure of the particles milled for 7 hours is similar to that of the 4 hours milled sample, with more layers.

The sample milled for 10 hours has the most layers amongst all the samples. However, it is observed to be more homogenous and refined due to increasing cold welding.

After milling the magnesium-nickel powder for 15 hours and beyond a reduction in the particle size is observed with a significant amount of refinement. At this stage, the particles have very less layers and due to the influence of cold welding a much more homogenous structure of the particles is observed.

SEM images of the samples milled for different ball milling times reveal that as the milling time increases the average particle size reduces as shown in Fig 4.15.

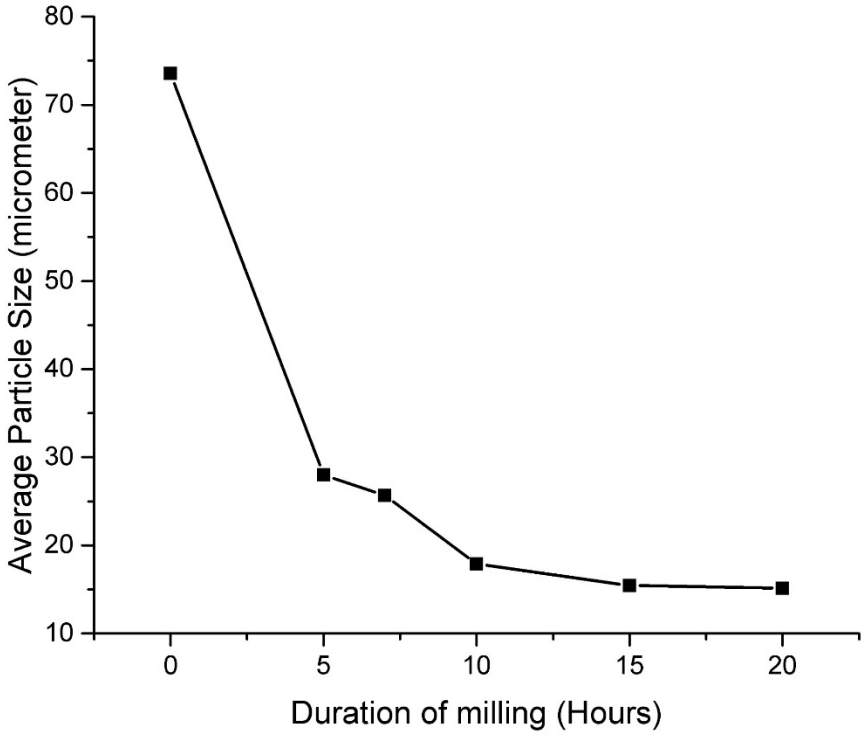

Figure 4.17. Variation of average particle size by changing the duration of milling.

A substantial reduction in the average particle size is observed from 0 – 10 hours of milling. After 10 hours of milling, particle size still reduces but the change is minimal. This can justify the fact that Mg-10wt%Ni ball milled for 10 hours stores more hydrogen when compared to the one which has been milled for only 5 hours as there would be lesser number of cracks induced in a bigger particle. Also, because of the observed layered structure the effective surface area of the particles would be the highest in Mg-10wt%Ni, facilitating more reaction sites for the hydrogen atoms.
When milled for 15 and 20 hours, the particle size gets smaller but the hydrogen capacity reduces because after a certain extent further particle size reduction leads to lesser hydrogen storage in the β-phase[11].

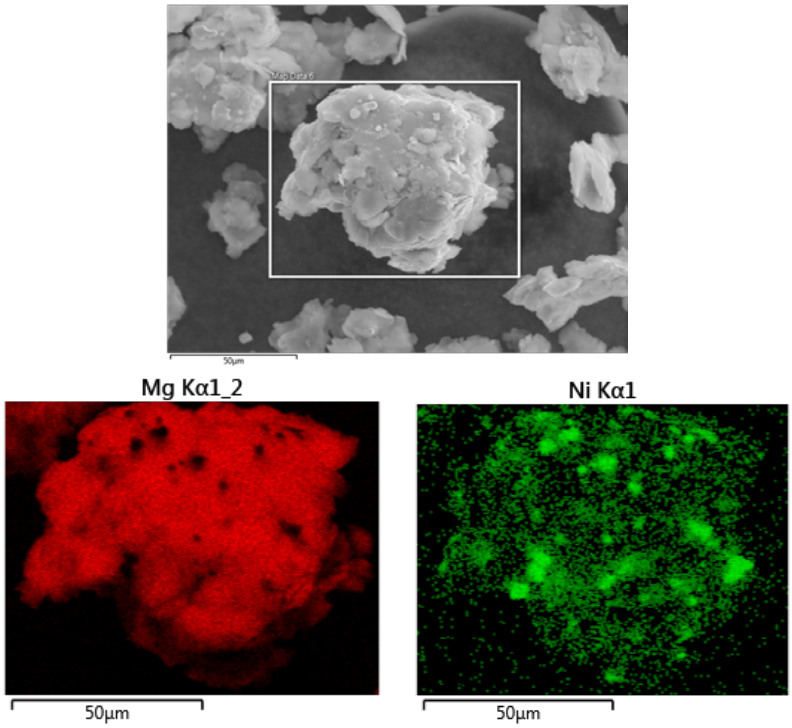

Figure 4.18. EDS scan of Mg-10wt%Ni ball milled for 5 hours.

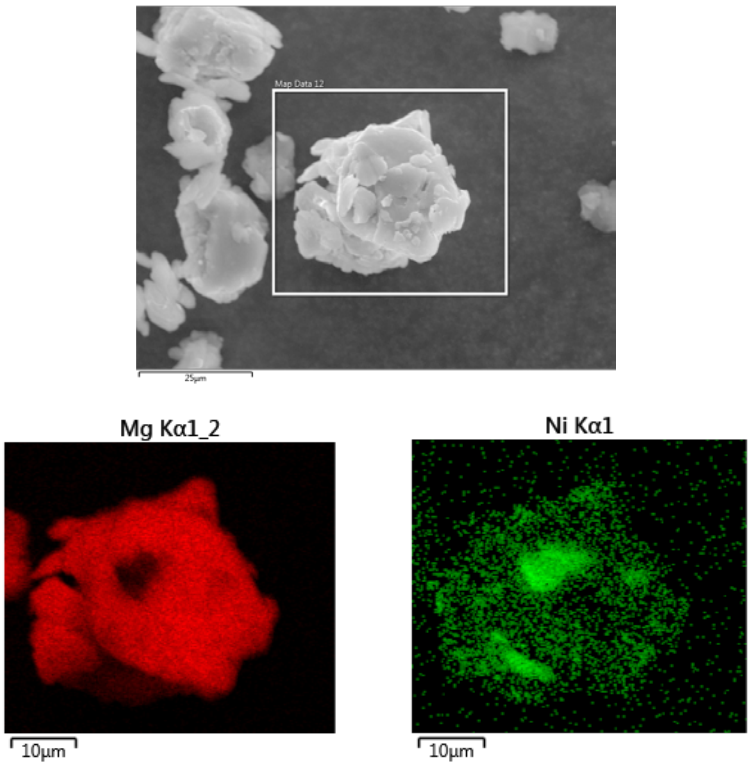

Figure 4.19. EDS scan of Mg-10wt%Ni ball milled for 7 hours.

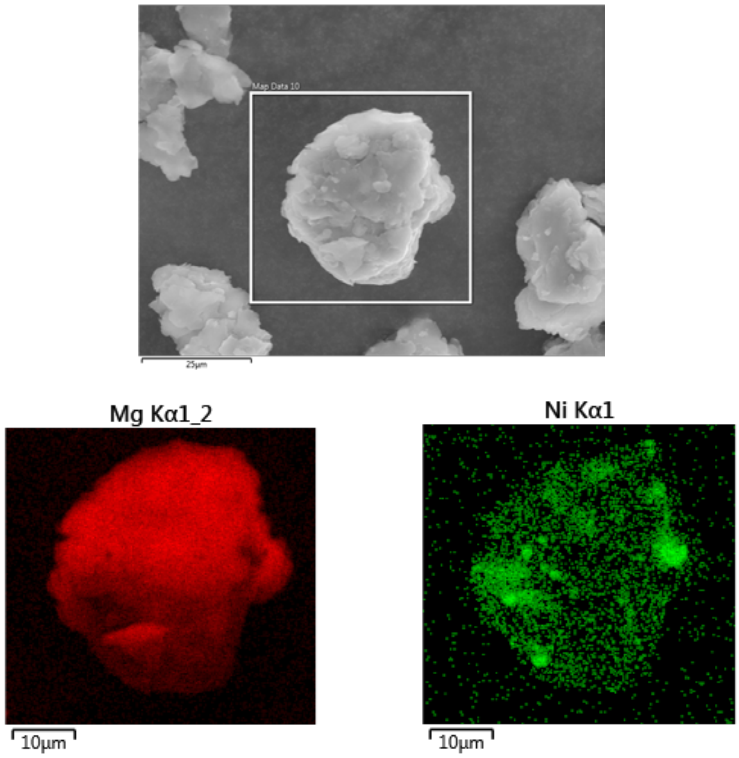

Figure 4.20. EDS scan of Mg-10wt%Ni ball milled for 10 hours.

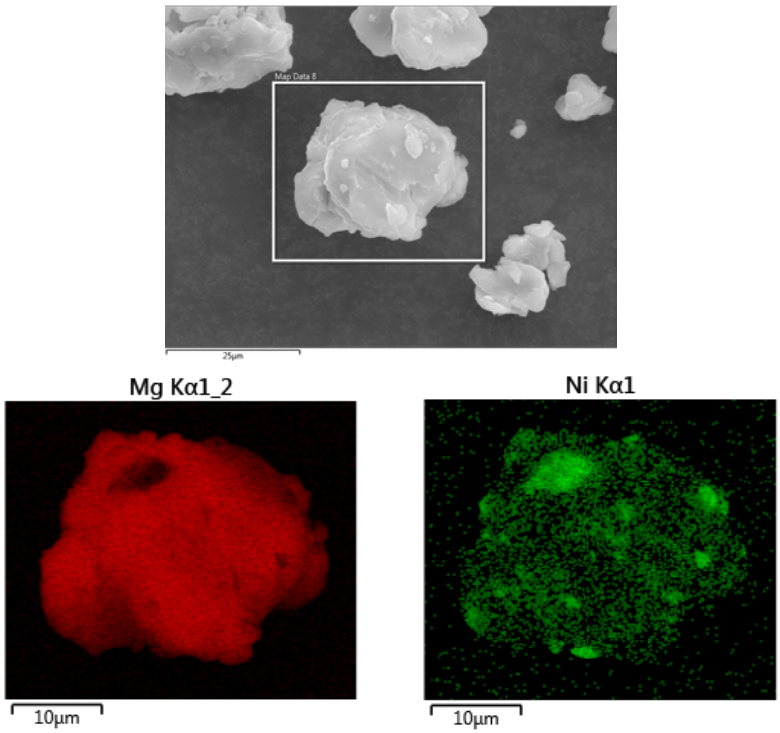

Figure 4.21. EDS scan of Mg-10wt%Ni ball milled for 15 hours.

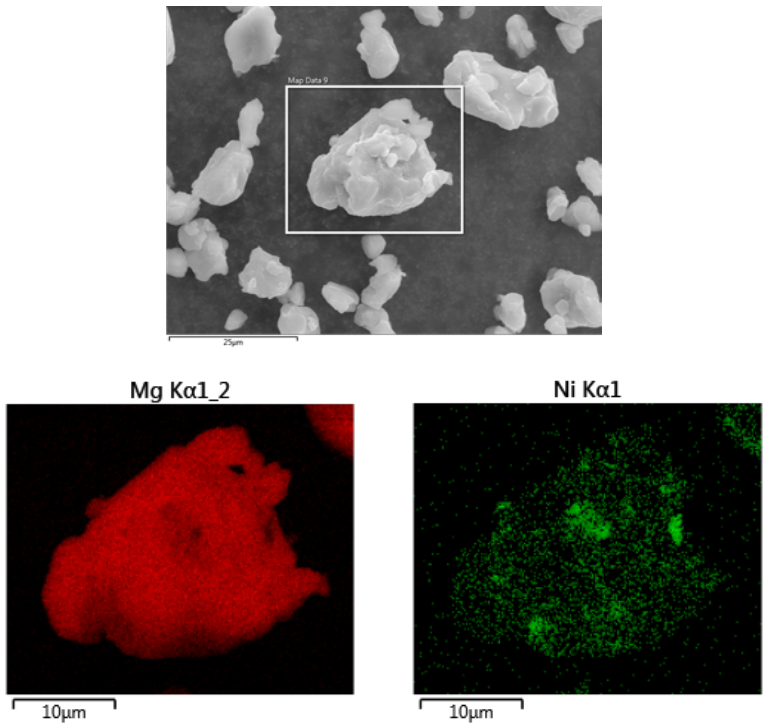

Figure 4.22. EDS scan of Mg-10wt%Ni ball milled for 20 hours.

EDS scans clearly show that as the ball milling duration is increased, more uniformly distributed and smaller particles of nickel are observed on the large chunk of magnesium powder. Figure 4.20 shows the most uniform distribution of nickel particles when ball milled for 20 hours.

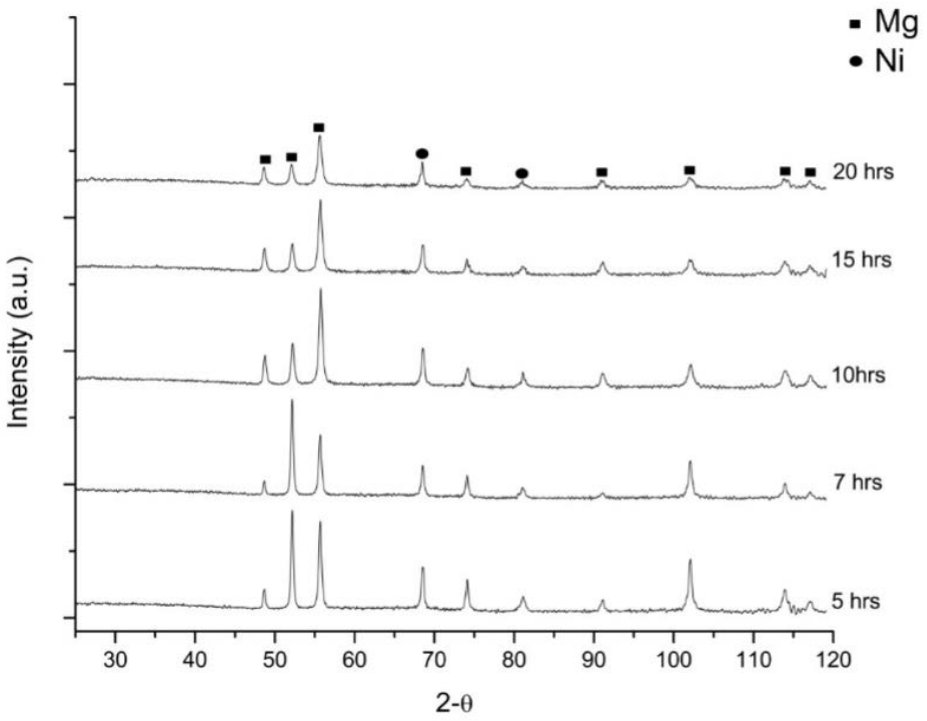

Figure 4.23. XRD scan of unhydrided Mg-10wt%Ni ball milled for different hours.

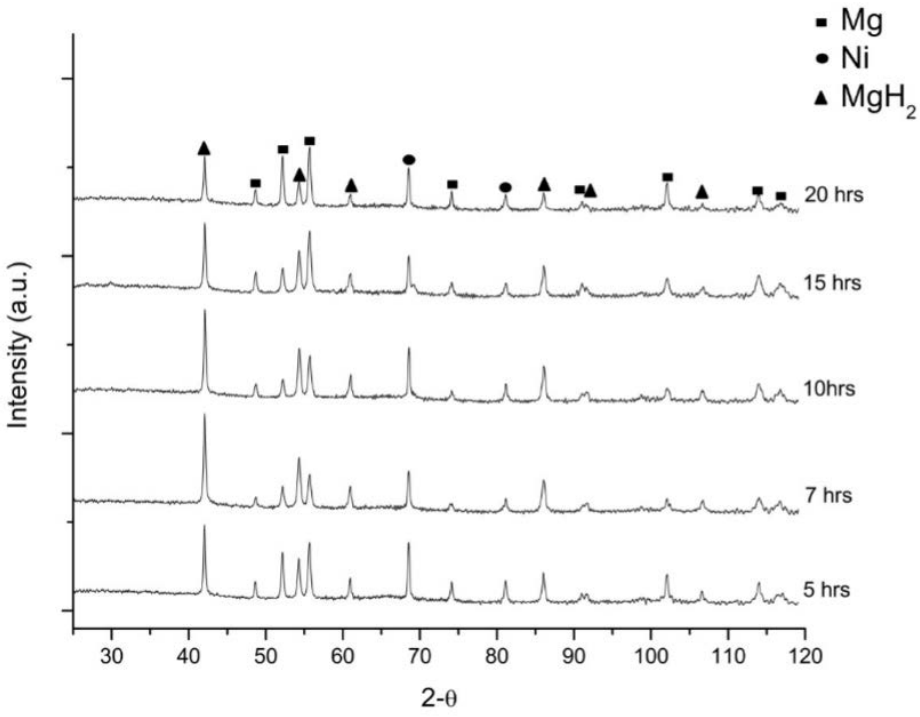

Figure 4.24. XRD scan of hydrided Mg-10wt%Ni ball milled for different hours.

Figure 4.21 and 4.22 show the X-ray diffraction scans for the unhydrided and the hydrided samples. It can be clearly seen that upon charging the samples with hydrogen at 20 bar and 300°C, the only phases existing were: Mg, Ni, MgH_2. Absence of Mg_2NIH_4 enhances the hydrogen storage capacity of the samples, as Mg_2NIH_4 has a hydrogen storage capacity of 3.6 wt% only.

4.3 Effect of varying absorption pressure on the hydrogen storage characteristics of magnesium-nickel alloy.

From the above two sections, it is evident that the most suitable sample was Mg-10wt%Ni ball milled for 10 hours. For see the effect of absorption pressure, Mg-10wt%Ni was charged with hydrogen at 300°C and different pressures: 5, 10, 15, 20 and 25 bar.

Again, results were obtained using a flowmeter and a desorption temperature of 350°C and atmospheric pressure.

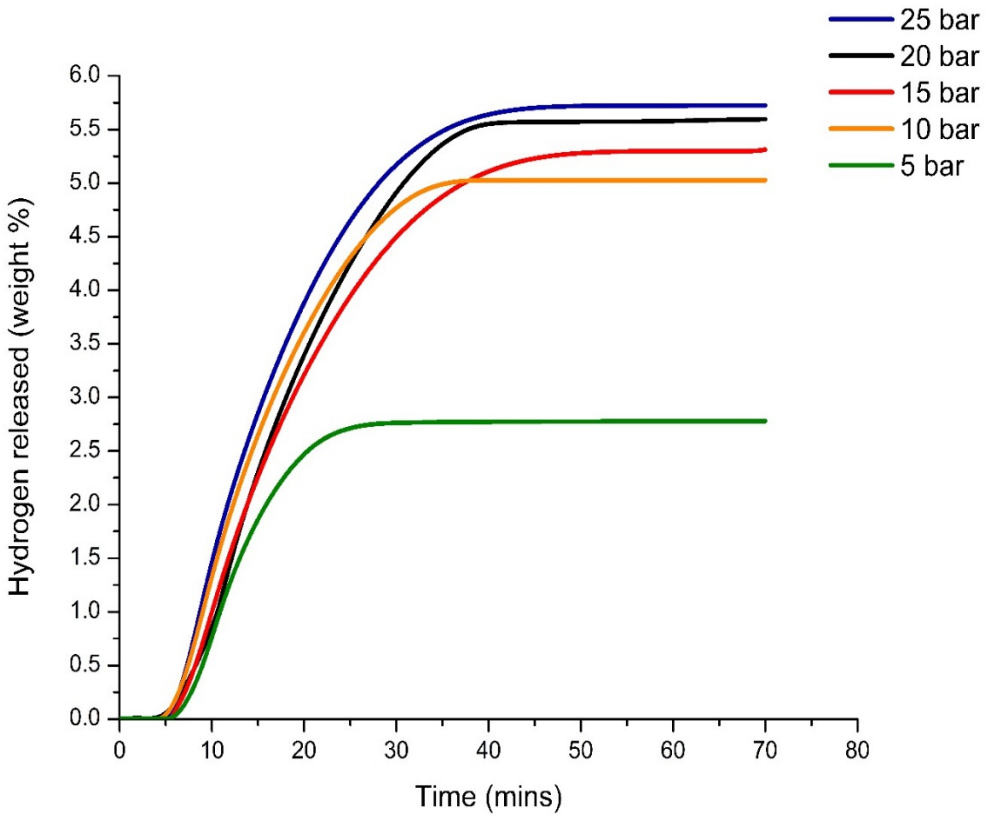

Figure 4.25. Effect of varying absorption pressure on the hydrogen storage capacity of Magnesium-10wt%Nickel milled for 10 hours.

Samples charged at different hydrogen pressures were discharged at 350°C. A substantial difference in the hydrogen storage capacity of the samples charged at 5 bar and 10 bar can be seen clearly from Fig 4.23. The hydrogen storage capacity is observed to increase substantially with

increase in the hydrogen charging pressure. However, a minimal difference (≈0.1wt%) in the hydrogen discharge is observed between the samples charged for 20 bar and 25 bar. The sample charged at a hydrogen pressure of 20 bar has faster reaction rates as compared to the sample charged at 25 bar. Therefore, Mg-10wt%Ni charged at 20 bar of pressure is the best suited sample.

4.4 Effect of varying absorption temperature on the hydrogen storage characteristics of magnesium-nickel alloy.

Mg-10wt%Ni ball milled for 10 hours was charged at 20 bar of hydrogen pressure and different temperatures: 250°C, 300°C, 350°C.

Samples were again discharged at 350°C and the outflow of hydrogen was measured using a flowmeter.

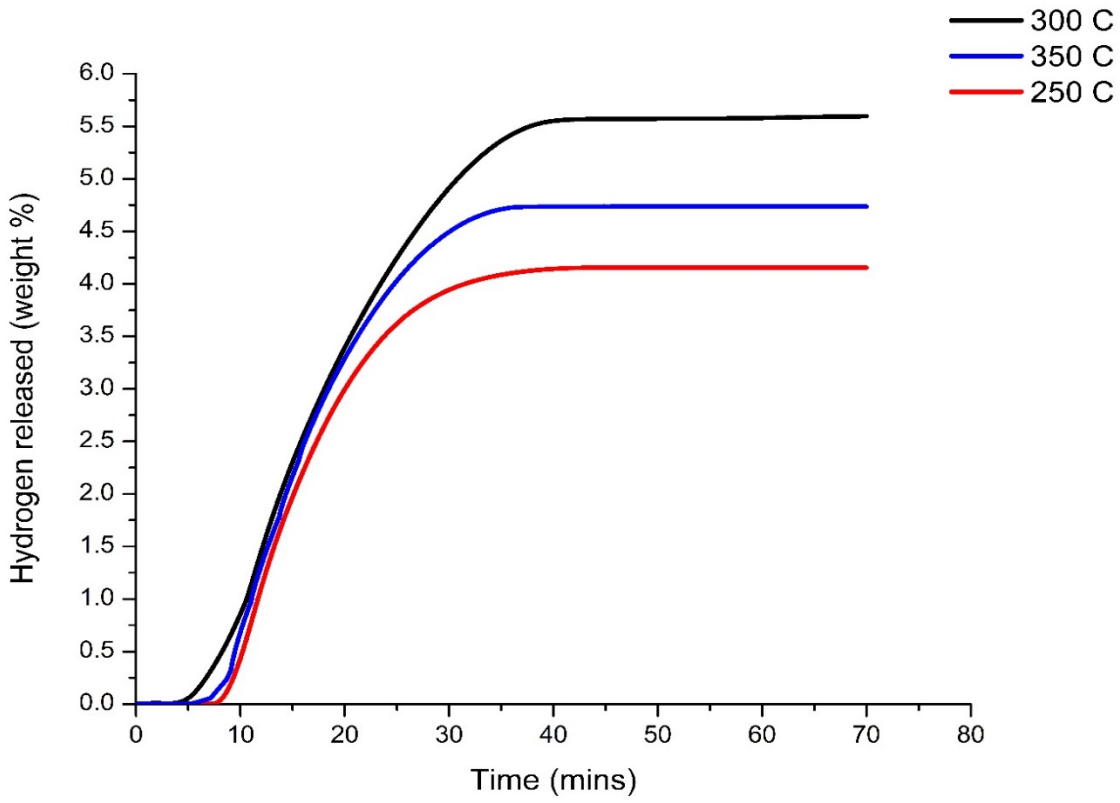

Figure 4.26. Effect of varying absorption temperature on the hydrogen storage capacity of Magnesium-10wt%Nickel milled for 10 hours.

The sample charged at a temperature of 300°C clearly shows to release the highest amount of hydrogen (≈5.6wt%). Increasing the charging temperature further to 350°C resulted in a degradation of the hydrogen storage capacity. Hydriding is suppressed at high temperatures and results in local consolidation of the hydride. Upon heating at high temperatures, the nanostructure and cyclability is highly degraded [11]. The sample charged at 350°C however, shows slightly faster discharging rate.

CHAPTER 5

CONCLUSIONS AND FUTURE WORK

5.1 Conclusion

The effect of ball milling, nickel content, hydrogen charging pressure, charging and discharging temperature on the hydrogen storage characteristics of Mg was studied. The purpose of ball milling was to induce cracks into the Magnesium particles to facilitate the residence of hydrogen atoms. Hydrogen storage and the rate of reaction was considered the main criterion to evaluate the progress of the experiments. Finally, the particle morphology, size and the distribution of nickel in magnesium were studied.

The first objective of this research was to obtain the desired composition of Nickel (in weight %) in the ball milled magnesium to achieve the best possible hydrogen storage characteristics. The results show that the particle size of magnesium reduced with the addition of nickel. The particle size reduced from 73.55µm (as-received) to 17.398µm (when 15wt% of Nickel was added). The particle size of the milled powder is of significant importance as it to a certain degree determines the available surface area of the particles for the reaction. SEM images revealed that all the samples had a laminated and layered structure formed by cold welding of flattened magnesium and nickel particles. These layers increased the effective surface area needed for the hydrogen to bond with the metal. The hydrogen storage tests revealed that the highest hydrogen storage amount (5.6wt%) does not correspond to the powder with the highest amount of nickel (Mg-15wt%Ni), but to the sample with 10wt% of hydrogen due to less amount of magnesium present in Mg-15wt%Ni.

The second objective was to obtain the most suitable ball milling time to achieve the best possible hydrogen storage characteristics. The results show that the particles size of magnesium reduced significantly upon ball milling. The particle size of the as-received sample was 73.55 μm, which reduced to 15.14 μm after ball milling for 20 hours. However, the hydrogen measurement test revealed that the highest hydrogen storage rate does not correspond to the finest powder (20 hours), but to the powder which was milled for 10 hours. SEM and EDS scans revealed the uniform distribution of nickel particles over larger magnesium particles with increasing milling time. After milling for 10 hours the Mg-Ni powders had a laminated structure with layers. This laminated structure could be responsible for more hydrogen stored in the sample due to the increased effective area. X-ray diffraction scans confirmed the absence of Mg_2NiH_4 and the presence of only Mg, Ni and MgH_2 after hydriding.

Table 5.1. Complete Summary of the results obtained

Nickel (wt%)	**Milling time (hours)**	**Pressure (bar)**	**Temperature (Celsius)**	**Hydrogen stored (wt%)**	**Discharging time (minutes)**
0	10	20	300	1.9	>70
1	10	20	300	2.6	55
5	10	20	300	4.7	45
7	10	20	300	5.2	43
10	10	20	300	5.6	35
15	10	20	300	5.3	50
10	5	20	300	5	55
10	7	20	300	5.6	60
10	15	20	300	2.8	25
10	20	20	300	2.6	28
10	10	5	300	2.7	25
10	10	15	300	5.2	50
10	10	25	300	5.64	48
10	10	20	250	4	43
10	10	20	350	4.6	35

The final phase of this research was to obtain the desired hydrogen charging pressure and temperature to achieve the best hydrogen storage characteristics. The highest amount of hydrogen was stored by Mg10wt%Ni sample charged with hydrogen at 25bar. However, the most suitable sample was the one charged at a hydrogen pressure of 20 bars as the difference in the hydrogen storage capacity was very small (< 0.1wt%).

Upon hydriding the samples at different temperatures and a constant pressure of 20 bar, the sample charged at 300°C stored the highest amount of hydrogen.

5.2 Future Works

- The different phases of the samples at different parameters were observed before and after hydriding with the help of X ray diffractometer. However, the intermediate phases formed during the hydriding and dehydriding process were not identified. It would be of interest to see the in-situ X-ray diffraction scan which can reveal the intermediate phases formed during the reaction.

- The EDS and SEM scans revealed the distribution of nickel particles on the magnesium surface. However, it would be of great interest to see the cross-sectional EDS and SEM scan of these samples, to better understand the internal structure of these particles.

- A future work can consider testing other samples with the same methodology by adding a different catalyst.

- A future work can consider testing other samples by reactive ball milling with hydrogen.

REFERENCES

[1] IEA, *World Energy Outlook 2007: China and India Insights*. 2007.

[2] U. D. of Energy, "Hydrogen Storage," *Fuel Cell Technol. Progr.*, p. 2, 2011.

[3] N. Takeichi *et al.*, "'Hybrid hydrogen storage vessel', a novel high-pressure hydrogen storage vessel combined with hydrogen storage material," *Int. J. Hydrogen Energy*, vol. 28, no. 10, pp. 1121–1129, 2003.

[4] W. P. Limited, *Solid-state hydrogen storage*, vol. 12, no. 5. 2009.

[5] G. Sandrock, "Panoramic overview of hydrogen storage alloys from a gas reaction point of view," *J. Alloys Compd.*, vol. 293, pp. 877–888, 1999.

[6] Y. Li and R. T. Yang, "Gas Adsorption and Storage in Metal-Organic Framework MOF-177on and Storage in Metal-Organic Framework MOF-177," *Langmuir*, vol. 23, no. 26, pp. 12937–12944, 2007.

[7] E. Poirier *et al.*, "Storage of hydrogen on single-walled carbon nanotubes and other carbon structures," *Appl. Phys. A*, vol. 78, no. 7, pp. 961–967, 2004.

[8] H. W. Langmi *et al.*, "Hydrogen storage in ion-exchanged zeolites," *J. Alloys Compd.*, vol. 404–406, no. SPEC. ISS., pp. 637–642, 2005.

[9] X. Lin *et al.*, "High H2 adsorption by coordination-framework materials," *Angew. Chemie - Int. Ed.*, vol. 45, no. 44, pp. 7358–7364, 2006.

[10] P. M. Budd *et al.*, "The potential of organic polymer-based hydrogen storage materials.," *Phys. Chem. Chem. Phys.*, vol. 9, pp. 1802–1808, 2007.

[11] V. Bérubé, G. Radtke, M. Dresselhaus, and G. Chen, "Size effects on the hydrogen storage properties of nanostructured metal hydrides: A review," *International Journal of Energy Research*, vol. 31, no. 6–7. pp. 637–663, 2007.

[12] L. Schlapbach and a Züttel, "Hydrogen-storage materials for mobile applications.," *Nature*, vol. 414, no. 6861, pp. 353–358, 2001.

[13] A. San-Martin and F. D. Manchester, "The H− Mg (Hydrogen-Magnesium) system," *J. phase equilibria*, vol. 8, no. 5, pp. 431–437, 1987.

[14] T. Noritake *et al.*, "Chemical bonding of hydrogen in MgH2," *Appl. Phys. Lett.*, vol. 81, no. 11, pp. 2008–2010, 2002.

[15] A. R. Vijay Babu, N. Devunuri, D. R. Manisha, Y. Prashanthi, R. Merugu, and A. J. R.

Ravi Teja, “Magnesium hydrides for hydrogen storage: A mini review,” *Int. J. ChemTech Res.*, vol. 6, no. 7, pp. 3451–3455, 2014.

[16] L. Takacs and J. S. McHenry, “Temperature of the milling balls in shaker and planetary mills,” in *Journal of Materials Science*, 2006, vol. 41, no. 16, pp. 5246–5249.

[17] R. K. Rajamani, P. Songfack, and B. K. Mishra, “Impact energy spectra of tumbling mills,” *Powder Technol.*, vol. 108, no. 2–3, pp. 116–121, 2000.

[18] W. Cao, “Synthesis of Nanomaterials by high energy ball milling,” *Skyspring Nanomaterials, Inc*, 2016. [Online]. Available: http://www.understandingnano.com/nanomaterial-synthesis-ball-milling.html.

[19] J. Yang, M. Ciureanu, and R. Roberge, “Hydrogen storage properties of nano-composites of Mg and Zr-Ni-Cr alloys,” *Mater. Lett.*, vol. 43, no. 5, pp. 234–239, 2000.

[20] J. Huot, G. Liang, S. Boily, A. Van Neste, and R. Schulz, “Structural study and hydrogen sorption kinetics of ball-milled magnesium hydride,” *J. Alloys Compd.*, vol. 293, pp. 495–500, 1999.

[21] J. J. Vajo, F. Mertens, C. C. Ahn, R. C. Bowman, and B. Fultz, “Altering hydrogen storage properties by hydride destabilization through alloy formation: LiH and MgH 2 destabilized with Si,” *J. Phys. Chem. B*, vol. 108, no. 37, pp. 13977–13983, 2004.

[22] P. C. H. Mitchell, a J. Ramirez-Cuesta, S. F. Parker, J. Tomkinson, and D. Thompsett, “Hydrogen spillover on carbon-supported metal catalysts studied by inelastic neutron scattering. Surface vibrational states and hydrogen riding modes,” *J. Phys. Chem. B*, vol. 107, no. 28, pp. 6838–6845, 2003.

[23] P. Hjort, a. Krozer, and B. Kasemo, “Hydrogen sorption kinetics in partly oxidized Mg films,” *J. Alloys Compd.*, vol. 237, no. 1–2, pp. 74–80, 1996.

[24] K. Yoshimura, Y. Yamada, and M. Okada, “Hydrogenation of Pd capped Mg thin films at room temperature,” *Surf. Sci.*, vol. 566–568, no. 1–3 PART 2, pp. 751–754, 2004.

[25] A. Zaluska, L. Zaluski, and J. O. Str??m-Olsen, “Nanocrystalline magnesium for hydrogen storage,” *J. Alloys Compd.*, vol. 288, no. 1–2, pp. 217–225, 1999.

[26] L. Zaluski, A. Zaluska, and J. . Ström-Olsen, “Nanocrystalline metal hydrides,” *J. Alloys Compd.*, vol. 253–254, pp. 70–79, 1997.

[27] F. Zeppelin, H. Reule, and M. Hirscher, “Hydrogen desorption kinetics of nanostructured MgH2 composite materials,” in *Journal of Alloys and Compounds*, 2002, vol. 330–332,

pp. 723–726.

[28] N. Hanada, T. Ichikawa, and H. Fujii, “Catalytic effect of nanoparticle 3d-transition metals on hydrogen storage properties in magnesium hydride MgH2 prepared by mechanical milling,” *J. Phys. Chem. B*, vol. 109, no. 15, pp. 7188–7194, 2005.

[29] J. Charbonnier *et al.*, “Hydrogenation of transition element additives (Ti, V) during ball milling of magnesium hydride,” in *Journal of Alloys and Compounds*, 2004, vol. 383, no. 1–2, pp. 205–208.

[30] Z. Dehouche *et al.*, “Influence of cycling on the thermodynamic and structure properties of nanocrystalline magnesium based hydride,” *J. Alloys Compd.*, vol. 305, no. 1–2, pp. 264–271, 2000.

[31] G. Liang, J. Huot, S. Boily, A. Van Neste, and R. Schulz, “Hydrogen storage properties of the mechanically milled MgH2-V nanocomposite,” *J. Alloys Compd.*, vol. 291, no. 1–2, pp. 295–299, 1999.

[32] J. L. Bobet, B. Chevalier, M. Y. Song, and B. Darriet, “Improvements of hydrogen storage properties of Mg-based mixtures elaborated by reactive mechanical milling,” in *Journal of Alloys and Compounds*, 2003, vol. 356–357, pp. 570–574.

[33] M. Song, I. Kwon, S. Kwon, C. Park, H. Park, and J. S. Bae, “Preparation of hydrogen-storage alloy Mg-10 wt% Fe2O3 under various milling conditions,” *Int. J. Hydrogen Energy*, vol. 31, no. 1, pp. 43–47, 2006.

[34] R. L. Holtz and M. A. Imam, “Hydrogen storage characteristics of ball-milled magnesium-nickel and magnesium-iron alloys,” vol. 4, pp. 2655–2663, 1999.

[35] M. Y. Song, M. Pezat, B. Darriet, and P. Hagenmuller, “Hydriding mechanism of Mg2Ni in the presence of oxygen impurity in hydrogen,” *J. Mater. Sci.*, vol. 20, no. 8, pp. 2958–2964, 1985.

[36] L. Zaluski, A. Zaluska, and J. O. Ström-Olsen, “Hydrogen absorption in nanocrystalline Mg2Ni formed by mechanical alloying,” *J. Alloys Compd.*, vol. 217, no. 2, pp. 245–249, 1995.

[37] M. H. Mintz, Z. Gavra, and Z. Hadari, “Kinetic study of the reaction between hydrogen and magnesium, catalyzed by addition of indium,” *J. Inorg. Nucl. Chem.*, vol. 40, no. 5, pp. 765–768, 1978.

[38] M. Abdellaoui, D. Cracco, and A. Percheron-Guegan, “Structural characterization and

reversible hydrogen absorption properties of Mg2Ni rich nanocomposite materials synthesized by mechanical alloying," *J. Alloys Compd.*, vol. 268, no. 1–2, pp. 233–240, 1998.

[39] R. Vijay, R. Sundaresan, M. P. Maiya, and S. S. Murthy, "Comparative evaluation of Mg-Ni hydrogen absorbing materials prepared by mechanical alloying," *Int. J. Hydrogen Energy*, vol. 30, no. 5, pp. 501–508, 2005.

[40] A. K. S. A. links open the author workspace. A. K. S. A. links open the author workspace. O. N. Srivastava, "On the synthesis of the Mg2Ni alloy by mechanical alloying," *J. Alloys Compd.*, vol. 227, no. 1, pp. 63–68, 1995.

[41] M. Abdellaoui, S. Mokbli, F. Cuevas, M. Latroche, A. Percheron Guegan, and H. Zarrouk, "Structural, solid-gas and electrochemical characterization of Mg 2Ni-rich and MgxNi100-x amorphous-rich nanomaterials obtained by mechanical alloying," in *International Journal of Hydrogen Energy*, 2006, vol. 31, no. 2, pp. 247–250.

[42] G. Liang, S. Boily, J. Huot, A. Van Neste, and R. Schulz, "Mechanical alloying and hydrogen absorption properties of the Mg–Ni system," *J. Alloys Compd.*, vol. 267, no. 1–2, pp. 302–306, 1998.

[43] C. Zhou and J. A. Szpunar, "Hydrogen Storage Performance in Pd/Graphene Nanocomposites," *ACS Appl. Mater. Interfaces*, vol. 8, no. 39, pp. 25933–25940, 2016.

[44] W. A. Rachinger, "A correction for the alpha1 alpha2 Doublet in the Measurement of widths of X-ray Diffraction Lines," *J. Sci. Instrum.*, vol. 25, pp. 254–255, 1948.

[45] "Introduction to Energy Dispersive X-ray Spectrometry (EDS)." .

APPENDIX

COPYRIGHT PERMISSIONS

For the images, graphs or tables used that form a part of a thesis, written permission from the publisher (copyright holder) is required by the College of Graduate Studies and Research (CGSR). This appendix includes the copyright permissions from the publishers for the images, graphs and tables that were published or are under review, and used in this thesis.

Copyright permission for Figure 2.1

This Agreement between Mr. Bhaskar Paliwal ("You") and Nature Publishing Group ("Nature Publishing Group") consists of your license details and the terms and conditions provided by Nature Publishing Group and Copyright Clearance Center.

License Number	4150920268423
License date	Jul 16, 2017
Licensed Content Publisher	Nature Publishing Group
Licensed Content Publication	Nature
Licensed Content Title	Hydrogen-storage materials for mobile applications
Licensed Content Author	Louis Schlapbach and Andreas Zuttel
Licensed Content Date	Nov 15, 2001
Licensed Content Volume	414
Licensed Content Issue	6861
Type of Use	reuse in a dissertation / thesis
Requestor type	academic/educational
Format	print and electronic
Portion	figures/tables/illustrations

Number of figures/tables/illustrations	1
Figures	Potential energy curve for the Lennard-Jones potential
Author of this NPG article	no
Your reference number	
Title of your thesis / dissertation	Optimizing the production procedure of ball milled Magnesium-Nickel powders for hydrogen storage applications
Expected completion date	Aug 2017
Estimated size (number of pages)	70
Requestor Location	Mr. Bhaskar Paliwal 101 Cumberland Ave S Saskatoon, SK S7N1L5 Canada Attn: Mr. Bhaskar Paliwal
Billing Type	Invoice
Billing Address	Mr. Bhaskar Paliwal 101 Cumberland Ave S Saskatoon, SK S7N1L5 Canada Attn: Mr. Bhaskar Paliwal
Total	0.00 CAD

Terms and Conditions

Terms and Conditions for Permissions

Nature Publishing Group hereby grants you a non-exclusive license to reproduce this material for this purpose, and for no other use,subject to the conditions below:

NPG warrants that it has, to the best of its knowledge, the rights to license reuse of this material. However, you should ensure that the material you are requesting is original to Nature Publishing Group and does not carry the copyright of another entity (as credited in the published version). If the credit line on any part of the material you have requested indicates that it was reprinted or adapted by NPG with permission from another source, then you should also seek permission from that source to reuse the material.

Permission granted free of charge for material in print is also usually granted for any electronic version of that work, provided that the material is incidental to the work as a whole and that the electronic version is essentially equivalent to, or substitutes for, the print version.Where print permission has been granted for a fee, separate permission must be obtained for any additional, electronic re-use (unless, as in the case of a full paper, this has already been accounted for during your initial request in the calculation of a print run).NB: In all cases, web-based use of full-text articles must be authorized separately through the 'Use on a Web Site' option when requesting permission.

Permission granted for a first edition does not apply to second and subsequent editions and for editions in other languages (except for signatories to the STM Permissions Guidelines, or where the first edition permission was granted for free).

Nature Publishing Group's permission must be acknowledged next to the figure, table or abstract in print. In electronic form, this acknowledgement must be visible at the same time as the figure/table/abstract, and must be hyperlinked to the journal's homepage.

The credit line should read:
Reprinted by permission from Macmillan Publishers Ltd: [JOURNAL NAME] (reference citation), copyright (year of publication)
For AOP papers, the credit line should read:
Reprinted by permission from Macmillan Publishers Ltd: [JOURNAL NAME], advance online publication, day month year (doi: 10.1038/sj.[JOURNAL ACRONYM].XXXXX)

Note: For republication from the *British Journal of Cancer*, the following credit lines apply.
Reprinted by permission from Macmillan Publishers Ltd on behalf of Cancer Research UK: [JOURNAL NAME] (reference citation), copyright (year of publication)For AOP papers, the credit line should read:
Reprinted by permission from Macmillan Publishers Ltd on behalf of Cancer Research UK: [JOURNAL NAME], advance online publication, day month year (doi: 10.1038/sj.[JOURNAL ACRONYM].XXXXX)

Adaptations of single figures do not require NPG approval. However, the adaptation should be credited as follows:

Adapted by permission from Macmillan Publishers Ltd: [JOURNAL NAME] (reference citation), copyright (year of publication)

Note: For adaptation from the *British Journal of Cancer*, the following credit line applies.
Adapted by permission from Macmillan Publishers Ltd on behalf of Cancer Research UK: [JOURNAL NAME] (reference citation), copyright (year of publication)

Translations of 401 words up to a whole article require NPG approval. Please visit http://www.macmillanmedicalcommunications.com for more information.Translations of up to a 400 words do not

require NPG approval. The translation should be credited as follows:

Translated by permission from Macmillan Publishers Ltd: [JOURNAL NAME] (reference citation), copyright (year of publication).

Note: For translation from the *British Journal of Cancer*, the following credit line applies.
Translated by permission from Macmillan Publishers Ltd on behalf of Cancer Research UK: [JOURNAL NAME] (reference citation), copyright (year of publication)

We are certain that all parties will benefit from this agreement and wish you the best in the use of this material. Thank you.

Copyright permission for Table 2.1 and Figure 2.3

Order Number	501288756
Order date	Jul 16, 2017
Licensed Content Publisher	Elsevier
Licensed Content Publication	Elsevier Books
Licensed Content Title	Solid-State Hydrogen Storage
Licensed Content Author	Gavin Walker
Licensed Content Date	2008
Licensed Content Volume	n/a
Licensed Content Issue	n/a

Licensed Content Pages	1
Start Page	xvii
End Page	xviii
Type of Use	reuse in a thesis/dissertation
Intended publisher of new work	other
Portion	figures/tables/illustrations
Number of figures/tables/illustrations	2
Format	both print and electronic
Are you the author of this Elsevier chapter?	No
Will you be translating?	No
Order reference number	
Original figure numbers	Table 1.2
Title of your thesis/dissertation	Optimizing the production procedure of ball milled Magnesium-Nickel powders for hydrogen storage applications
Expected completion date	Aug 2017
Estimated size (number of pages)	70
Elsevier VAT number	GB 494 6272 12
Requestor Location	Mr. Bhaskar Paliwal 101 Cumberland Ave S Saskatoon, SK S7N1L5 Canada Attn: Mr. Bhaskar Paliwal
Total	Not Available

Terms and Conditions for Permissions

Nature Publishing Group hereby grants you a non-exclusive license to reproduce this material for this purpose, and for no other use,subject to the conditions below:

NPG warrants that it has, to the best of its knowledge, the rights to license reuse of this material. However, you should ensure that the material you are requesting is original to Nature Publishing Group and does not carry the copyright of another entity (as credited in the published version). If the credit line on any part of the material you have requested

indicates that it was reprinted or adapted by NPG with permission from another source, then you should also seek permission from that source to reuse the material.

Permission granted free of charge for material in print is also usually granted for any electronic version of that work, provided that the material is incidental to the work as a whole and that the electronic version is essentially equivalent to, or substitutes for, the print version.Where print permission has been granted for a fee, separate permission must be obtained for any additional, electronic re-use (unless, as in the case of a full paper, this has already been accounted for during your initial request in the calculation of a print run).NB: In all cases, web-based use of full-text articles must be authorized separately through the 'Use on a Web Site' option when requesting permission.

Permission granted for a first edition does not apply to second and subsequent editions and for editions in other languages (except for signatories to the STM Permissions Guidelines, or where the first edition permission was granted for free).

Nature Publishing Group's permission must be acknowledged next to the figure, table or abstract in print. In electronic form, this acknowledgement must be visible at the same time as the figure/table/abstract, and must be hyperlinked to the journal's homepage.

The credit line should read:
Reprinted by permission from Macmillan Publishers Ltd: [JOURNAL NAME] (reference citation), copyright (year of publication)
For AOP papers, the credit line should read:
Reprinted by permission from Macmillan Publishers Ltd: [JOURNAL NAME], advance online publication, day month year (doi: 10.1038/sj.[JOURNAL ACRONYM].XXXXX)

Note: For republication from the *British Journal of Cancer*, the following credit lines apply.
Reprinted by permission from Macmillan Publishers Ltd on behalf of Cancer Research UK: [JOURNAL NAME] (reference citation), copyright (year of publication)For AOP papers, the credit line should read:
Reprinted by permission from Macmillan Publishers Ltd on behalf of Cancer Research UK: [JOURNAL NAME], advance online publication, day month year (doi: 10.1038/sj.[JOURNAL ACRONYM].XXXXX)

Adaptations of single figures do not require NPG approval. However, the adaptation should be credited as follows:

Adapted by permission from Macmillan Publishers Ltd: [JOURNAL NAME] (reference citation), copyright (year of publication)

Note: For adaptation from the *British Journal of Cancer*, the following credit line applies.
Adapted by permission from Macmillan Publishers Ltd on behalf of Cancer Research UK: [JOURNAL NAME]

(reference citation), copyright (year of publication)

Translations of 401 words up to a whole article require NPG approval. Please visit http://www.macmillanmedicalcommunications.com for more information.Translations of up to a 400 words do not require NPG approval. The translation should be credited as follows:

Translated by permission from Macmillan Publishers Ltd: [JOURNAL NAME] (reference citation), copyright (year of publication).

Note: For translation from the *British Journal of Cancer*, the following credit line applies.
Translated by permission from Macmillan Publishers Ltd on behalf of Cancer Research UK: [JOURNAL NAME] (reference citation), copyright (year of publication)

We are certain that all parties will benefit from this agreement and wish you the best in the use of this material. Thank you.

Copyright permission for Figure 3.1

Title: Hydrogen Storage Performance in Pd/Graphene Nanocomposites

Author: Chunyu Zhou, Jerzy A. Szpunar

Publication: Applied Materials

Publisher: American Chemical Society

Date: Oct 1, 2016

PERMISSION/LICENSE IS GRANTED FOR YOUR ORDER AT NO CHARGE

This type of permission/license, instead of the standard Terms & Conditions, is sent to you because no fee is being charged for your order. Please note the following:

Permission is granted for your request in both print and electronic formats, and translations.
If figures and/or tables were requested, they may be adapted or used in part.
Please print this page for your records and send a copy of it to your publisher/graduate school.

Appropriate credit for the requested material should be given as follows: "Reprinted (adapted) with permission from (COMPLETE REFERENCE CITATION). Copyright (YEAR) American Chemical Society." Insert appropriate information in place of the capitalized words.
One-time permission is granted only for the use specified in your request. No additional uses are granted (such as derivative works or other editions). For any other uses, please submit a new request.

If credit is given to another source for the material you requested, permission must be obtained from that source.

Copyright permission for Figure 2.1, 2.2, 2.5

This Agreement between Mr. Bhaskar Paliwal ("You") and John Wiley and Sons ("John Wiley and Sons") consists of your license details and the terms and conditions provided by John Wiley and Sons and Copyright Clearance Center.

License Number	4151020863012
License date	Jul 16, 2017
Licensed Content Publisher	John Wiley and Sons
Licensed Content Publication	International Journal of Energy Research
Licensed Content Title	Size effects on the hydrogen storage properties of nanostructured metal hydrides: A review
Licensed Content Author	Vincent Bérubé,Gregg Radtke,Mildred Dresselhaus,Gang Chen
Licensed Content Date	Mar 14, 2007
Licensed Content Pages	27
Type of use	Dissertation/Thesis
Requestor type	University/Academic
Format	Print and electronic

Portion	Figure/table
Number of figures/tables	3
Original Wiley figure/table number(s)	Figure 1, Figure 2, Figure 6
Will you be translating?	No
Title of your thesis / dissertation	Optimizing the production procedure of ball milled Magnesium-Nickel powders for hydrogen storage applications
Expected completion date	Aug 2017
Expected size (number of pages)	70
Requestor Location	Mr. Bhaskar Paliwal 101 Cumberland Ave S Saskatoon, SK S7N1L5 Canada Attn: Mr. Bhaskar Paliwal
Publisher Tax ID	EU826007151
Billing Type	Invoice
Billing Address	Mr. Bhaskar Paliwal 101 Cumberland Ave S Saskatoon, SK S7N1L5 Canada Attn: Mr. Bhaskar Paliwal
Total	0.00 CAD

Terms and Conditions

TERMS AND CONDITIONS

This copyrighted material is owned by or exclusively licensed to John Wiley & Sons, Inc. or one of its group companies (each a"Wiley Company") or handled on behalf of a society with which a Wiley Company has exclusive publishing rights in relation to a particular work (collectively "WILEY"). By clicking "accept" in connection with completing this licensing transaction, you agree that the following terms and conditions apply to this transaction (along with the billing and payment terms and conditions established by the

Copyright Clearance Center Inc., ("CCC's Billing and Payment terms and conditions"), at the time that you opened your RightsLink account (these are available at any time at http://myaccount.copyright.com).

Terms and Conditions

The materials you have requested permission to reproduce or reuse (the "Wiley Materials") are protected by copyright.

You are hereby granted a personal, non-exclusive, non-sub licensable (on a stand-alone basis), non-transferable, worldwide, limited license to reproduce the Wiley Materials for the purpose specified in the licensing process. This license, **and any CONTENT (PDF or image file) purchased as part of your order,** is for a one-time use only and limited to any maximum distribution number specified in the license. The first instance of republication or reuse granted by this license must be completed within two years of the date of the grant of this license (although copies prepared before the end date may be distributed thereafter). The Wiley Materials shall not be used in any other manner or for any other purpose, beyond what is granted in the license. Permission is granted subject to an appropriate acknowledgement given to the author, title of the material/book/journal and the publisher. You shall also duplicate the copyright notice that appears in the Wiley publication in your use of the Wiley Material. Permission is also granted on the understanding that nowhere in the text is a previously published source acknowledged for all or part of this Wiley Material. Any third party content is expressly excluded from this permission.

With respect to the Wiley Materials, all rights are reserved. Except as expressly granted by the terms of the license, no part of the Wiley Materials may be copied, modified, adapted (except for minor reformatting required by the new Publication), translated, reproduced, transferred or distributed, in any form or by any means, and no derivative works may be made based on the Wiley Materials without the prior permission of the respective copyright owner.**For STM Signatory Publishers clearing permission under the terms of the STM Permissions Guidelines only, the terms of the license are extended to include subsequent editions and for editions in other languages, provided such**

editions are for the work as a whole in situ and does not involve the separate exploitation of the permitted figures or extracts,You may not alter, remove or suppress in any manner any copyright, trademark or other notices displayed by the Wiley Materials. You may not license, rent, sell, loan, lease, pledge, offer as security, transfer or assign the Wiley Materials on a stand-alone basis, or any of the rights granted to you hereunder to any other person.

The Wiley Materials and all of the intellectual property rights therein shall at all times remain the exclusive property of John Wiley & Sons Inc, the Wiley Companies, or their respective licensors, and your interest therein is only that of having possession of and the right to reproduce the Wiley Materials pursuant to Section 2 herein during the continuance of this Agreement. You agree that you own no right, title or interest in or to the Wiley Materials or any of the intellectual property rights therein. You shall have no rights hereunder other than the license as provided for above in Section 2. No right, license or interest to any trademark, trade name, service mark or other branding ("Marks") of WILEY or its licensors is granted hereunder, and you agree that you shall not assert any such right, license or interest with respect thereto

NEITHER WILEY NOR ITS LICENSORS MAKES ANY WARRANTY OR REPRESENTATION OF ANY KIND TO YOU OR ANY THIRD PARTY, EXPRESS, IMPLIED OR STATUTORY, WITH RESPECT TO THE MATERIALS OR THE ACCURACY OF ANY INFORMATION CONTAINED IN THE MATERIALS, INCLUDING, WITHOUT LIMITATION, ANY IMPLIED WARRANTY OF MERCHANTABILITY, ACCURACY, SATISFACTORY QUALITY, FITNESS FOR A PARTICULAR PURPOSE, USABILITY, INTEGRATION OR NON-INFRINGEMENT AND ALL SUCH WARRANTIES ARE HEREBY EXCLUDED BY WILEY AND ITS LICENSORS AND WAIVED BY YOU.

WILEY shall have the right to terminate this Agreement immediately upon breach of this Agreement by you.

You shall indemnify, defend and hold harmless WILEY, its Licensors and their respective directors, officers, agents and employees, from and against any actual or threatened claims, demands, causes of action or proceedings arising from any breach of this Agreement by you.

IN NO EVENT SHALL WILEY OR ITS LICENSORS BE LIABLE TO YOU OR ANY OTHER PARTY OR ANY OTHER PERSON OR ENTITY FOR ANY SPECIAL, CONSEQUENTIAL, INCIDENTAL, INDIRECT, EXEMPLARY OR PUNITIVE DAMAGES, HOWEVER CAUSED, ARISING OUT OF OR IN CONNECTION WITH THE DOWNLOADING, PROVISIONING, VIEWING OR USE OF THE MATERIALS REGARDLESS OF THE FORM OF ACTION, WHETHER FOR BREACH OF CONTRACT, BREACH OF WARRANTY, TORT, NEGLIGENCE, INFRINGEMENT OR OTHERWISE (INCLUDING, WITHOUT LIMITATION, DAMAGES BASED ON LOSS OF PROFITS, DATA, FILES, USE, BUSINESS OPPORTUNITY OR CLAIMS OF THIRD PARTIES), AND WHETHER OR NOT THE PARTY HAS BEEN ADVISED OF THE POSSIBILITY OF SUCH DAMAGES. THIS LIMITATION SHALL APPLY NOTWITHSTANDING ANY FAILURE OF ESSENTIAL PURPOSE OF ANY LIMITED REMEDY PROVIDED HEREIN.

Should any provision of this Agreement be held by a court of competent jurisdiction to be illegal, invalid, or unenforceable, that provision shall be deemed amended to achieve as nearly as possible the same economic effect as the original provision, and the legality, validity and enforceability of the remaining provisions of this Agreement shall not be affected or impaired thereby.

The failure of either party to enforce any term or condition of this Agreement shall not constitute a waiver of either party's right to enforce each and every term and condition of this Agreement. No breach under this agreement shall be deemed waived or excused by either party unless such waiver or consent is in writing signed by the party granting such waiver or consent. The waiver by or consent of a party to a breach of any provision of this

Agreement shall not operate or be construed as a waiver of or consent to any other or subsequent breach by such other party.

This Agreement may not be assigned (including by operation of law or otherwise) by you without WILEY's prior written consent.

Any fee required for this permission shall be non-refundable after thirty (30) days from receipt by the CCC.

These terms and conditions together with CCC's Billing and Payment terms and conditions (which are incorporated herein) form the entire agreement between you and WILEY concerning this licensing transaction and (in the absence of fraud) supersedes all prior agreements and representations of the parties, oral or written. This Agreement may not be amended except in writing signed by both parties. This Agreement shall be binding upon and inure to the benefit of the parties' successors, legal representatives, and authorized assigns.

In the event of any conflict between your obligations established by these terms and conditions and those established by CCC's Billing and Payment terms and conditions, these terms and conditions shall prevail.

WILEY expressly reserves all rights not specifically granted in the combination of (i) the license details provided by you and accepted in the course of this licensing transaction, (ii) these terms and conditions and (iii) CCC's Billing and Payment terms and conditions.

This Agreement will be void if the Type of Use, Format, Circulation, or Requestor Type was misrepresented during the licensing process.

This Agreement shall be governed by and construed in accordance with the laws of the State of New York, USA, without regards to such state's conflict of law rules. Any legal action, suit or proceeding arising out of or relating to these Terms and Conditions or the breach thereof shall be instituted in a court of competent jurisdiction in New York County in the State of New York in the United States of America and each party hereby consents and submits to the personal jurisdiction of such court, waives any objection to venue in

such court and consents to service of process by registered or certified mail, return receipt requested, at the last known address of such party.

WILEY OPEN ACCESS TERMS AND CONDITIONS

Wiley Publishes Open Access Articles in fully Open Access Journals and in Subscription journals offering Online Open. Although most of the fully Open Access journals publish open access articles under the terms of the Creative Commons Attribution (CC BY) License only, the subscription journals and a few of the Open Access Journals offer a choice of Creative Commons Licenses. The license type is clearly identified on the article.

The Creative Commons Attribution License

The Creative Commons Attribution License (CC-BY) allows users to copy, distribute and transmit an article, adapt the article and make commercial use of the article. The CC-BY license permits commercial and non-

Creative Commons Attribution Non-Commercial License

The Creative Commons Attribution Non-Commercial (CC-BY-NC)License permits use, distribution and reproduction in any medium, provided the original work is properly cited and is not used for commercial purposes.(see below)

Creative Commons Attribution-Non-Commercial-NoDerivs License

The Creative Commons Attribution Non-Commercial-NoDerivs License (CC-BY-NC-ND) permits use, distribution and reproduction in any medium, provided the original work is properly cited, is not used for commercial purposes and no modifications or adaptations are made. (see below)

Use by commercial "for-profit" organizations

Use of Wiley Open Access articles for commercial, promotional, or marketing purposes requires further explicit permission from Wiley and will be subject to a fee.

Further details can be found on Wiley Online Library http://olabout.wiley.com/WileyCDA/Section/id-410895.html